

**EFFECTS OF PYK2-DEFICIENCY ON MIDPALATAL
SUTURE EXPANSION IN MICE**

By

JUN SUN

Submitted to the Graduate Faculty of the School of
Dentistry in partial fulfillment of the requirements
for the degree of Master of Science in Dentistry,
Indiana University School of Dentistry, 2015

Thesis accepted by the Graduate Faculty of the division of Prosthodontics, Department of Restorative Dentistry, Indiana University School of Dentistry, in partial fulfillment of the requirements for the degree of Master of Science in Dentistry.

Sean Shih-Yao Liu

David T. Brown

Tien Min Chu

Angela Bruzzaniti

Chair of the Research Committee

John A. Levon

Program Director, Graduate Prosthodontics

Date

ACKNOWLEDGMENTS

I am deeply grateful to my supervisors, Dr. Angela Bruzzaniti and Dr. Sean Shih-Yao Liu, who have the attitude and the substance of genius. Without their valuable guidance, inspiring suggestion and persistent help, this dissertation would not have been possible.

A great thanks goes out to my department director, Dr. John Levon who provided me with a great chance to broaden my view of prosthodontics knowledge. His instruction, expertise and optimistic attitude encourage me to keep passion for work and life.

Appreciation also goes out to Carol Bain for her histotechnology support and for always being available to help.

I would like to express my sincere gratitude to my research committee, Dr. David T. Brown and Dr. Tien Min Chu for their invaluable assistance and support throughout my research.

I would also like to thank all faculty members and colleagues in the Graduate Prosthodontics Program at Indiana University School of Dentistry. Your kindness and friendship supported me throughout the journey.

I really appreciate the financial assistance by research grants from Dr. Angela Bruzzaniti (NIH R01 AR060332), Dr. Sean Shin-Yao Liu (Startup funding of IUSD 22-763-40) and Delta Dental foundation (2015 Dental Master's Thesis Award).

Finally, and most importantly, I would like to express appreciation to my beloved family. A special thanks to my husband, Dr. Li Zhan, who has given me an enormous amount of support and encouragement throughout my graduate study. My son, Jingqi Zhan, has been a great source of happiness and joy to me during the challenging times. I am also grateful for my parents and sister, who have shown their unconditional care and provision throughout my life. The love, support and patience from my beloved family will accompany and drive me to the bright future. I love you!

TABLE OF CONTENTS

INTRODUCTION	1
MATERIALS AND METHODS.....	13
RESULTS	20
TABLES	28
FIGURES	32
DISCUSSION.....	50
SUMMARY AND CONCLUSIONS	56
REFERENCES	58
ABSTRACT.....	62
ABBREVIATIONS	65
CURRICULUM VITAE.....	67

LIST OF TABLES

TABLE 1. Summary of tissue parameters for control and expanded mice	29
TABLE 2. Statistical analysis of mouse comparison.....	30
TABLE 3. Statistical analysis of expansion force comparison.....	31

LIST OF FIGURES

FIGURE 1. Occlusal view of midpalatal suture in 6-week-old mice.	33
FIGURE 2. Micro-CT images for measurement.....	34
FIGURE 3. Three dimensional micro-CT reconstructed images of control and expanded sutures.	35
FIGURE 4. The ratio of BV/TV from micro-CT analysis.....	36
FIGURE 5. Suture width from micro-CT analysis.	37
FIGURE 6. Maxilla width from micro-CT analysis.	38
FIGURE 7. Bone labeling of control and expanded midpalatal suture.	39
FIGURE 8. TRAP staining images of midpalatal suture.....	40
FIGURE 9. The ratio of Oc.S/ BS from TRAP staining.....	41
FIGURE 10. ALP stained images of midpalatal suture and the alveolar ridge of molar.	42
FIGURE 11. H&E stained images of the midpalatal suture.	43
FIGURE 12. The width of fibrous region from H&E staining.	44
FIGURE 13. The height of fibrous region from H&E staining.	45
FIGURE 14. The area of fibrous region from H&E staining.	46
FIGURE 15. Alcian Blue staining of cartilage and chondrocytes.....	47
FIGURE 16. The area of cartilage region in sutures.	48
FIGURE 17. Hypertrophic chondrocytes number.	49

INTRODUCTION

Bone homeostasis is dependent on the balanced actions of osteoclasts which resorb bone and osteoblasts which form new bone. A disruption of the bone remodeling process can lead to skeletal disorders including osteoporosis, arthritis and many inheritable skeletal diseases. Mechanical stresses generating from orthodontic appliances can lead to craniofacial bone remodeling and facial bony defects. In addition, defects in bone modelling or remodeling in the oral and craniofacial system may require orthognathic surgery as well as pharmacologic approaches for bone regeneration.

Suture expansion is a very important clinical approach to correct maxillary width deficiency but has a high potential of treatment relapse. Accelerating bone formation and mineralization in the mid-palatal suture during suture expansion may be beneficial in preventing relapse of the arch width and reducing the retention period. Pyk2-mediated signaling pathways are involved in osteoclast and osteoblast function. Pyk2 knock-out mice have augmented bone formation and bone mass, suggesting that therapeutic strategies that target Pyk2 may be useful to enhance bone remodeling and prevent suture relapse during suture expansion.

Purpose

In this study we examined the role of Pyk2 in bone formation and suture remodeling in the mid-palatal suture following rapid maxillary expansion. Pyk2 knock out (Pyk2-KO) and wild-type (WT) mice received no expansion (0 g), 10 g or 20 g force of rapid maxillary expansion for 14 days using nickel titanium spring expanders. Three dimensional (3D) morphometric analysis of the suture and histomorphometry were used

to detect changes in bone volume to total volume (BV/TV), bone formation rate as well as osteoclast and osteoblast activities *in vivo*.

Hypothesis

Our null hypothesis (H_0) was that there would be no difference in the mid-palatal suture bone mass between Pyk2-KO mice and WT mice following suture expansion. Our alternative hypothesis (H_A) was that Pyk2-KO mice would show increased mid-palatal suture bone mass following suture expansion.

REVIEW OF LIERATURE

Rapid maxillary expansion (RME) is an effective technique to increase the transverse dimension of the mid-face to correct posterior crossbite and relieve dental crowding with a narrow maxillary dental arch ^[1]. When the midpalatal suture opens, the maxillopalatine complex and surrounding tissues also receive expansion force, which can induce suture disjunction and increase bone remodeling in adjacent craniofacial sutures, resulting in an increase in the transverse dimension of the entire midface ^[2]. This technique uses an expander to separate the midpalatal suture, induce new bone deposition at the suture bone margins, and finally reach the goal of widening the maxillary arch.

Although rapid maxillary expansion (RME) is commonly used to open the midpalatal suture and widen constricted maxillary arches in orthodontics, it has a high tendency for treatment relapse. After expansion, soft and bony tissues within the suture exert resistance forces that tend to pull the two palatal shelves back to their original unexpanded position. Even though new bone forms at the suture margins, it is usually insufficient in density and quality (immature bone) to withstand the resistance force. To minimize relapse, a long retention period of 3 to 6 months is usually recommended to prevent relapse and allow new bone to grow and mature in the expanded suture. Ideally, increasing bone volume and mineral density in the expanded suture will likely shorten the retention period after expansion.

New bone formation during suture expansion occurs in two stages. During the first stage an initial traumatic response is followed by a period of connective tissue repair and wound healing. During the second stage, the new bone deposition occurs perpendicular or parallel to the bony edges of the suture in tension areas to re-establish the original bone morphology ^[3, 4]. Unfortunately, in RME, the rate of suture expansion often exceeds the

rate of bone formation within the suture. The prolonged suture gap leads to a high potential of treatment relapse because the connective tissues between the separated bones tend to pull the maxillary bones back into their original positions. This leads to the reduced treatment effects and requires an extensive retention period to decrease the rate of relapse ^[5]. A previous animal histologic study and a computed-tomography evaluation on patients have shown that the retention time for the reorganization and restoration of the bone density of suture tissue is at least 6 months ^[6, 7]. In order to shorten the retention period and obtain ideal treatment effects of RME in patients with constricted maxillary arches, strategies have to be employed to stimulate bone formation within the suture during RME treatment ^[1, 8, 9].

As joints, sutures unite bones, absorb and transmit mechanical stresses, and also play a role as growth sites adapt to the change of the local mechanical environment ^[3, 10]. Craniofacial sutures are subjected to loads from natural activities, such as intermittent force from mastication, cyclic loading from pulsation of blood vessels, and quasi-static force from growth of neighboring tissues ^[10]. The remodeling of suture and adjacent bones occurs in response to functional demands caused by mechanical loading ^[4, 11, 12]. Orthodontists commonly use expanders to open midpalatal sutures with mechanical forces to augment the maxillary width ^[13]. Hou et al. ^[14] demonstrated that bone formation was more active in the suture after application of the expansion force compared with that of the suture without any intervention. Moreover, expansion forces across the midpalatal suture promote bone resorption through activation of osteoclasts and bone formation by increasing proliferation and differentiation of periosteal osteoblast cells. Therefore, despite being applied exogenously, this orthodontic force will be

transmitted as mechanical stress and strain within the suture, which in turn will induce local gene expression and the differentiation, proliferation and matrix synthesis of osteoblasts and chondrocytes. Osteoclast activity within the suture is also required to enable sutural remodeling and growth ^[15].

The hard palate of a mouse contains three sutures from front to rear on the transverse plane; a midpalatal suture between the first and second molars, a transverse palatine suture, and an interpalatine suture at the posterior end ^[16]. These sutures allow the palate to grow in two directions; widen in the lateral direction (midpalatal and interpalatine sutures), and elongate in an anteroposterior direction (transverse palatine suture). There are significant differences in the tissue structure, bone density, and cell number among the three suture types. The midpalatal suture is an end-to-end suture in mouse. It is the least interdigitated among the three sutures and the most common area for suture expansion ^[13, 16]. The midpalatal suture mainly consists of unmineralized matrices, including polygonal mesenchymal cells, secondary cartilage and fibrous tissue in the middle zone between two cartilaginous areas ^[4, 17]. The existence of the unmineralized suture mesenchyme is essential for the continuous growth of the adjacent bones. The mesenchymal progenitor cells in unmineralized sutures have the capability to differentiate into fibrogenic, chondrogenic, and osteogenic lineages ^[12]. Mechanical force enhances the differentiation of mesenchymal cells in the suture ^[18, 19].

RME initiates a mild injury to the suture which is followed by a proliferative repair mechanism that begins soon after injury. Injury to connective tissue usually results in scar formation. However, within the suture, instead of forming scar tissue, fibroblast activity pulls the palatal shelves back to their original position, leading to suture relapse ^[4].

Secondary cartilages are also found in the sutures and cover the front edges of the rodent animal sutures. Secondary cartilage is chiefly composed of chondrocytes embedded in an extracellular matrix. The presence of secondary cartilages, as a resilient tissue, is regarded as a sutural adaptation to mechanical forces, such as compression, tension and shearing stresses ^[17, 18]. Bone tissue has a low tolerance for these types of force, and secondary cartilage could provide a degree of structural protection. Secondary cartilage also has the potential of endochondral ossification in suture ^[20].

Osteoblasts and osteoclasts are the two major bone cell types that regulate the bone remodeling process. Bone remodeling involves a balance between the bone formation by osteoblasts, and the bone destruction by osteoclasts. Unlike osteoblasts which differentiate from mesenchymal stem cells, osteoclasts are derived from the hematopoietic monocyte-macrophage lineage. The intercellular communication between osteoblasts and osteoclasts is very important for bone homeostasis and dysfunction in this process can lead to bone diseases. Osteoblasts play a key role in the differentiation and function of osteoclasts by producing several factors, such as receptor activator of the NF- κ B ligand (RANKL), macrophage colony stimulating factor (M-CSF), osteoprotegerin (OPG), interleukin-1 (IL-1) and tumor necrosis factor (TNF) ^[21, 22]. OPG is a secreted product and blocks the ability of RANKL to bind to the RANK receptor in osteoclasts, thereby reducing osteoclasts differentiation. Therefore, the RANKL/OPG ratio is critical regulator of osteoclast activity.

Skeletal tissues develop via two distinct pathways; intramembranous and endochondral ossification. Intramembranous ossification occurs when the pluripotent mesenchymal stem cells condense and become the osteoblast lineage and eventually

differentiate into osteoblasts. Another process of ossification is known as endochondral ossification. This process begins with a condensation of mesenchymal stem cells. The stem cells first differentiate into chondrocytes, form a rigid template of cartilage and are eventually replaced by osteoblasts ^[22]. In a growing plate of long bone, the cartilage template transforms into bone and includes a series of microscopic regions including the resting zone, proliferative zone, hypertrophic zone and ossification zone. The hypertrophic stage is the last stage of chondrocytes differentiation and is characterized by a large cell volume, low nucleus to cytoplasm ratio and active secretion of the cartilage matrix ^[23]. In general, the nasomaxillary bones develop and grow through intramembranous ossification ^[3]. However, endochondral ossification also plays a significant role in mandibular development, long bone formation and growth, as well as fracture healing.

When a tension force is applied, many cytokines regulating bone regeneration and remodeling, such as transforming growth factor- β (TGF- β), bone morphogenetic protein-2 (BMP-2) and vascular endothelial growth factor (VEGF), are secreted by cells present in the suture ^[22, 24]. These cytokines promote the bone repair process. In independent studies, Liu et al. ^[8] and Lai et al. ^[25] implanted absorbable collagen sponges containing recombinant human bone morphogenetic protein-s (rhBMP-2) over craniofacial sutures in rabbits or rats, respectively. Both laboratories found that rhBMP-2 promoted bone formation in the expanded suture and decreased the relapse ratio (the rate of decrease in distance). Lee et al. ^[26] reported that the relapse of mechanical sutural expansion was decreased by the injection of bisphosphonate (etidronate), an inhibitor of osteoclastic bone resorption, in rat sagittal sutures combined with mechanical retention.

Pharmaceutical aids may therefore be therapeutically beneficial to the inhibition of relapse and shortening of the retention period during rapid expansion. However, the application rhBMP-2 and bisphosphonate can lead to medical complications. The former may induce ectopic bone formation, osteolysis and suture fusion^[8, 27]; the latter may result in bisphosphonate-related osteonecrosis of the jaw^[28]. Therefore, there is a clinical need to find new ways to increase bone mass and bone formation in the suture.

The protein tyrosine kinase 2 (Pyk2) is a mediator of intracellular protein signaling pathways. It has been well established that genetic deletion or pharmacologic inhibition of Pyk2 regulates bone remodeling and improves osteogenesis^[29-31]. Pyk2 knock-out (Pyk2-KO) mice, which lack the *Pyk2* gene, have normal bone development but bone mass and bone formation are increased^[30, 32]. Compared to wild-type (WT) mice, Pyk2-KO mice demonstrated a significant increase in bone volume to total volume (BV/TV), trabecular number, trabecular thickness and trabecular volumetric bone mineral density (BMD) in both the distal femur and lumbar vertebrae^[29, 30].

The high bone mass of Pyk2-KO mice is due to both increased osteoblast activity as well decreased osteoclast activity^[30, 32]. Pyk2 is highly expressed in osteoclasts and localizes in the actin and integrin-rich adhesion domain known as the “sealing zone” following osteoclast adhesion^[29, 31, 33]. Pyk2-KO osteoclasts fail to form sealing zones and exhibit defects in bone resorption^[29, 31, 33]. Pyk2-deficiency also regulates the differentiation of early osteoprogenitor cells across species and affects both osteoblastogenesis and osteoblast activity^[30].

Osteoblast differentiation is a multi-step series associated with cell proliferation, matrix mineralization and matrix maturation^[34]. The matrix maturation phase is

characterized by maximal expression of alkaline phosphatase. Analysis of bone markers, such as alkaline phosphatase (ALP), osteocalcin and osteopontin, is frequently used to characterize osteoblasts activity^[35]. Young et al.^[36] found that under fluid shear stress, primary calvarial osteoblasts from Pyk2-KO mice showed increased c-Fos and COX-2 proteins, both of which play roles in bone remodeling by transcriptional activation of bone matrix proteins. Buckbinder et al.^[30] reported that daily administration of a pyrimidine-based Pyk2 inhibitor increased bone formation and blocked bone loss in rats. These studies indicate that under normal physiological conditions, Pyk2 exhibits an inhibitory effect on bone mass and further suggest that pharmacologic inhibition of Pyk2 may increase bone mass.

Currently, the role of Pyk2 in chondrocytes is not well defined. A limited number of reports suggest that the Pyk2-mediated pathway may regulate collagenase expression in chondrocytes *in vitro*. In two studies using chondrocytes grown *in vitro*, it was shown that chemical inhibitors of Pyk2 decreased matrix metalloproteinase (MMP) upregulation in response to fibronectin fragments, which are known to enhance cartilage damage^[37,38]. Although no studies have been reported for the role of Pyk2-mediated signaling pathway in mechanically stimulated chondrocytes, the focal adhesion kinase (FAK), which is highly related to Pyk2, has been shown to be activated by ultrasound-induced mechanostimulation^[39] and has been shown to be involved in chondrogenic progenitor cell migration and cartilage healing^[40].

Based on the above studies, we hypothesized that inhibition of Pyk2 may enhance suture bone formation under orthodontic mechanical stimuli. In the current study, we used global Pyk2-KO mice to study bone formation and suture remodeling in the

midpalatal suture created by rapid maxillary expansion. Custom manufactured nickel-titanium springs were used to open the midpalatal sutures in this study due to the unique properties of Ni-Ti alloy in shape memory and super-elasticity which allow the springs when deformed to return to their original configuration. Ni-Ti springs can dissipate and maintain a stable, constant force on the midpalatal suture rather than abrupt force from the stainless steel springs^[41]. Our studies suggest that inhibiting Pyk2 during RME may be beneficial in correcting bone loss and preventing relapse of the suture.

MATERIALS AND METHODS

Animal procedures

Pyk2-KO (-/-) mice were described previously^[29] and were generously provided by Pfizer (Groton, CT, USA). Mice were bred as heterozygotes and crossed to generate Pyk2-KO mice and WT littermates. Pyk2-KO mice have been backcrossed more than 10 generations onto a C57BL/6 background. Thirty-six Pyk2-KO and thirty-six WT 6-week-old male mice were used in this study, approximately weighing 22-25 grams each. The six-week-old mice were in growing phase, and their first and second maxillary molars were fully erupted. All Pyk2-KO and WT mice were randomly and evenly assigned to three force groups; 0 g (serve as controls), 10 g or 20 g expansion force groups (n=12 per group). The control group did not receive any intervention (0 g). The animals in the 10 g and 20 g force groups received spring expanders made of 0.008” and 0.010” nickel titanium (Ni-Ti) wires (G&H Orthodontics, Franklin, IN) to expand the mid-palatal suture, respectively. The two ends of spring were inserted between the first and second molars underneath the proximal contact points. The appliances were bonded bilaterally on the maxillary molars with light cured composite resin (Transbond, 3M Unitek, CA) (Fig. 1). Half of the mice in each group was used for histology analysis (n=6 per group); the other half was assigned for fluorescence analysis (n=6 per group). Each animal was injected with alizarin complexone (MP Biomedical, Solon, OH) at 25 mg/kg body weight on day 1 and calcein (Sigma, St. Louis, MO) at 20 mg/kg body weight on day 11. All the bone labels were given once a day by intraperitoneal injection.

All mice were fed with the same ground diet and housed throughout the experiment in environmentally controlled rooms at Indiana University School of Dentistry Bioresearch Facility. Mice were euthanized on day 14 after suture expansion. The animal

procedures (DS000885R and DS0000916R) were reviewed and approved by the Institutional Animal Care and Use Committee of Indiana University School of Dentistry.

Tissue processing

The maxillae including midpalatal suture were dissected and fixed with 10% buffered formalin phosphate, which contains 4% formaldehyde (Fisher Scientific, Fair Lawn, NJ), for 7 days before X-ray imaging. After micro-CT scanning, thirty-six fixed specimens without bone labels were demineralized in 10% neutralized ethylenediaminetetraacetic acid (EDTA, PH 7.4) for 14 days and embedded in paraffin for histological study. Another thirty-six undecalcified maxillae injected with bone labels were embedded in methyl methacrylate (MMA) resin for fluorescence study.

Micro computed tomography scanning

The fixed intact maxillae were wrapped in paraffin and affixed to the scanning stage. These samples were scanned using high-resolution micro computed tomography at a resolution of 8 μm pixel size (Skyscan 1172, Kontich, Belgium). The system was set at a source of 59kV/167 μA , rotation angle of 180° with a rotation step of 0.45 °. Projection images were reconstructed using the NRecon software (Version 1.6.3.2, SkyScan).

Three dimensional micro computed tomography analysis

3D morphometric analyses (Ctan software, Version 1.10.1.0, SkyScan) were performed by selecting the palatal bone regions to obtain the bone volume fraction. The regions of interest (ROI) of suture consisted of the midpalatal suture bony edges, as well

as their bilateral extensions for 200 μm on each side with anterior and posterior boundaries at the notches of the palatal process (Fig. 2-A and B). The suture width (or remaining suture gap after expansion) was measured by tracing the two bony edges of the midpalatal suture using Image Pro Plus software (Version 6.0.0.260; Media Cybernetics, Bethesda, MD) (Fig. 2-C). The width of the maxillary bone was measured as the distance between canals of palatal roots of the right and left first molars using same software (Fig. 2-D).

Fluorescence analysis

The maxillae embedded in MMA resin were cut at 5 μm along the coronal plane between the first and second maxillary molars. The sections were viewed and the images were taken with a fluorescence microscope (Nikon DXM1200, Melville, NY) with 40X magnification.

Histomorphometry

Serial 5- μm -thick paraffin-embedded sections of decalcified maxillae were made in the coronal plane in the same area as the fluorescence analysis. These sections were used for Hematoxylin and Eosin staining (H&E) for morphological analyses, Tartrate Resistant Acid Phosphatase (TRAP) staining, Alkaline Phosphatase (ALP) detection and Alcian blue staining for visualizing the osteoclasts, osteogenesis and chondrocytes, respectively.

H&E staining is a routine histological technique to demonstrate tissue structures and condition. H&E stained sections were observed for morphological alterations under an

inverted microscope system (Leica DMI 4000B, Leica microsystems), and the microscopic photographs were taken at 50X and 100X magnification. The changes of suture morphology were compared among different types of mice and expansion forces. The width, height and area of fibrous region in the midpalatal suture were measured by tracing the interface of chondrocytes and fiber tissue using Image Pro Plus software. The width was defined between parallel chondrocytes of front bone edges. The height was measured between nasal side and oral side chondrocytes. The area was the whole fibrous region surrounded by chondrocytes.

TRAP is a metalloprotein enzyme, highly expressed in osteoclasts. TRAP stain was detected by using a histochemical procedure described by Erlebacher A^[42]. Osteoclasts, the multinucleated TRAP-positive cells appearing in the whole ROI, as previously defined in the coronal plane of the micro-CT images, were counted under the same Leica inverted microscope at high magnification (100X). The ratio of the bone surface area in direct contact with osteoclasts versus the total bone surface area (osteoclast surface/bone surface; Oc.S/BS) in each ROI was calculated using Bioquant Osteo software (Bioquant Image Analysis Corporation, Nashville, TN).

ALP is the most widely recognized biochemical marker for osteoblast activity and plays a role in bone formation. ALP expressions were examined by immunohistochemistry (IHC) using rabbit anti-mouse ALPL antibody (TA307702, OriGene Technologies, Rockville, MD) according to the manufacturer's instructions. Briefly, the serial sections from each sample were boiled for 3 minutes in 10 mM citrate buffer (PH 6.0) to retrieve the antigens. Then the sections were blocked with 3% goat serum (MP Biomedicals, Auckland, New Zealand) for 30 minutes at room temperature,

incubated overnight at 4°C with anti-mouse ALPL at 1:400 dilution. The signals were visualized after incubation with a secondary detection system (DAB 150 kit, Millipore, Billerica, MA). Normal goat serum used as the substitution of primary antibody for negative control did not reveal any signals (figure not shown). The photomicrographs of ALP signal on midpalatal suture and periodontal tissue were detected using the Leica microscope.

Alcian blue staining can detect proteoglycans (PGs), sulfated and carboxylated acid mucopolysaccharides, which are important in the production of the extracellular matrix of chondrocytes and cartilaginous elements. Alcian blue staining was used to detect the cartilage area and hypertrophic chondrocytes following the protocol described by Sheehan DC^[43]. The cartilage area was defined as the metachromatic regions on alcian blue stained sections and measured using Image Pro Plus software. Hypertrophic chondrocytes have unique phenotypic traits, large and round. The hypertrophic chondrocyte numbers were counted under the Leica microscope.

Statistical analysis

With a sample size of 6 mice per level of expansion force for the Pyk2-KO and WT mice, our study was predicted to have an 80% power to detect a difference of 3% in measurements. Two-way ANOVA was used to evaluate the effects of different magnitudes of expansion force on suture width, maxilla width, the ratio of bone volume to tissue volume, the ratio of the bone surface area in direct contact with osteoclasts versus the total bone surface area, the width, height and area of fibrous tissue, the cartilage area and hypertrophic chondrocyte number. Student T-test comparisons were

used for comparing differences between Pyk2-KO and WT mice among force levels. The differences were considered statistically significant at $p < 0.05$. Statistical support was provided by Elizabeth Moser, Biostatistician, School of Public Health.

RESULTS

General effects of suture expansion in mice.

In the current study, custom manufactured nickel-titanium springs were used to open the midpalatal sutures. Ni-Ti alloy exhibit the properties of shape memory and super-elasticity which allow the springs when deformed to return to their original configuration. We chose two expansion forces of 10 g and 20 g. We confirmed the force exerted by the compressed/activated springs using a digital force gauge (Lutron FG-5000, Lutron Electronic Enterprise Co., Taipei, Taiwan). The trans-palatal distance (measured between the left and right interproximal contacts of the maxillary first and second molars) was 3.8 μm in both the WT and Pyk2-KO groups. Three activated springs from the 10g group delivered $10\pm 1\text{g}$ force while 2 springs from the 20 g group delivered $20\pm 2\text{g}$ force.

During the 14 day experimental period, the springs were generally well tolerated by mice and no long-term adverse systemic reactions were observed. Mice were fed soft chow for the entire study and after an initial mild weight loss in the first few days following expansion, feeding and weight gain appeared normal.

Micro-CT analysis reveals increased bone mass in control and expanded Pyk2-KO mice.

Three dimensional (3D) reconstructions of WT and Pyk2-KO skulls after 14 days of expansion are shown in Figure 3. Panel A shows the occlusal view of the skull without midpalatal suture expansion while Panel C shows the skull with expansion. Panels B and D are high magnification images of the midpalatal suture area. The sutures following expansion are shown in Panels C and D. The transverse micro-CT images showed midpalatal, transverse and interpalatine sutures connected in the palate (Fig. 3-E).

Although the main purpose of the expander was to open the midpalatal suture, the expansion forces affected all three sutures. After expansion, the suture bony edge appeared loose in both genotypes of mice with increased suture width and broadened periodontal membrane space of molars (Fig. 3-F).

BV/TV is used to evaluate relative changes in bone volume density between different specimens or following a given treatment. The BV/TV ratio reflects the change in the size of bone marrow cavities. In this study, the total volume (TV) was defined by outlining ROI in the palatal bone, the bone volume (BV) was occupied by mineralized bone. The BV/TV ratio in Pyk2-KO mice was significantly higher ($p < 0.0001$) than the ratio in WT mice with and without expansion force (Table 1, Fig. 4). Under 10 g or 20 g expansion forces, there was a significant reduction in BV/TV in WT mice ($p < 0.05$) compared with control groups (0 g), whereas the 10 g force did not significantly decrease the BV/TV of Pyk2-KO mice ($p > 0.05$) (Table 2, Fig 4). Our data revealed that the BV/TV ratio of Pyk2-KO mice was decreased in both the 10 g group (-6 %) and 20 g force group (-11%). In WT mice, the loss of BV/TV was greater than in Pyk2-KO mice; BV/TV decreased -11% and -22% in the 10 g and the 20 g force groups. These data demonstrate that Pyk2-KO mice have higher bone mass before and after expansion, which may indicate higher resistance to the expansion forces than WT mice.

Expanded Pyk2-KO mice exhibited lower suture width and maxilla width compared to expanded WT mice.

The goal of RME is to increase maxilla width without excessive increase in suture width which would promote relapse. Micro-CT analysis showed that the suture width

was significantly increased in both mice genotypes receiving springs. In WT mice, the suture width was increased 5.3-fold and 6.4-fold in the 10 g and 20 g force groups, respectively ($p < 0.05$) (Table 2 and 3, Fig. 5). However, in Pyk2-KO mice, 10 g and 20 g springs only increased suture width 4.3-fold and 5.7-fold, respectively, compared to the 0 g force group.

After suture expansion, the maxilla widths of both WT and Pyk2-KO mice were significantly increased compared with non-treated (0 g) animals ($p < 0.0001$), confirming that RME was successful in our mice. Although maxilla width increased in both mice with the 10 g and 20 g, Pyk2-KO mice exhibited overall narrower maxillae than WT mice (Table 2, Fig. 6). In addition, we found no difference in maxilla width using the 10 g or 20 g springs in either mouse genotype.

Fluorescence analysis failed to show alizarin staining around sutures.

To determine the bone formation rate in the suture, we injected two fluorescent dyes which bind calcium which can be used to indicate the sites of mineralization, including the site of bone formation. Alizarin complexone (red) and calcein (green) were administered at day 1 and day 11, respectively. In the non-treated control group, the alizarin complexone red and calcein green labels were barely detected along the bony edges of midpalatal sutures. After suture expansion, the suture region was widened, new bone was formed at the front edges of sutures, and irregular suture bone margins were labeled by green. In the fluorescence images, there were strong calcein green labels along the sutures, which indicated active bone formation under expansion force. Furthermore, diffused calcein green labels were observed on the oral side and nasal side of sutures

where chondrocytes concentrated. However the Alizarin complexone red labels were too weak to be observed around suture edges (Fig. 7), most likely due to a high rate of bone turnover in the suture resulting in loss of the alizarin label. Therefore, we were unable to calculate the inter-label distance between the two injection time points which enables determination of the bone deposition rate (bone formation rate) in control and expanded mice.

TRAP staining shows decreased osteoclast number in Pyk2-KO after expansion.

To examine whether the increased BV/TV of Pyk2-KO mice following suture expansion was due to decreased osteoclast activity, maxillary bone sections were stained for TRAP, a marker of osteoclast activity. The osteoclast surface to bone surface (Oc.S/BS) ratio was then determined. Few multinucleated TRAP-positive cells were observed in the non-treated group of either Pyk2-KO or WT mice (Fig. 8). There was no significant difference in Oc.S/BS between Pyk2-KO and WT non-treated mice (Table 2, Fig. 9). In WT mice, Oc.S/BS was increased to 176% and 232% in the 10 g and 20 g force groups ($p < 0.05$), respectively, after 14 days of expansion (Table 3, Fig. 9). In contrast, in Pyk2-KO mice, the Oc.S/BS ratio was 127% and 134% in the 10 g and 20 g force groups ($p > 0.05$), respectively. These findings suggest that osteoclast differentiation and osteoclast number is lower in Pyk2-KO mice following expansion.

ALP expression appears to be increased by expansion force in WT mice.

Since alkaline phosphatase (ALP) is a bone marker of osteoblast maturation, we performed immunohistochemistry to determine the role of Pyk2 on osteoblast activity

following suture expansion. However, due to antibody-related technical difficulties that arose in specimen preparation, we were unable to quantitate the changes in ALP activity and osteoblast surface to bone surface (Ob.S/BS) in our bone specimens. Nevertheless, qualitative image analysis revealed an apparent increase in the number of ALP-positive cells after suture expansion. The number of ALP-positive cells in the suture regions of WT groups also appeared to be higher than in Pyk2-KO mice (Fig. 10). The alveolar ridge of molars in the 20 g expansion groups of Pyk2-KO and WT mice also revealed increased bone formation.

Decreased fibrous area in Pyk2-KO mice in the 10 g expansion force group

H&E staining, which is used to recognize various tissue types and suture morphologic changes, revealed a thin layer of fibrous tissue between chondrocytes, which covered the front bone edges of sutures (Fig. 11). In the expansion groups, the midpalatal sutures were broadened. Spindle-shaped fibroblasts and fibrous tissue occupied the suture gap between the chondrocyte layers and were arranged parallel to the expansion force. On the oral side of sutures, new bone was located adjacent to the periosteum and was covered by numerous chondrocytes. In contrast, on the nasal side of sutures, new bone was located next to the nasal epithelium and only a thin layer of chondrocytes was observed. In addition, the bone marrow cavities were extended and increased in the palatal bone. Pyk2-KO mice exhibited a reduced bone marrow area compared to WT mice with the same expansion force (Fig. 11).

It is well established that after suture expansion, fibroblasts differentiate from mesenchymal cells and proliferate in central zone of suture. However, the fibrous tissues

formed increases the rate of relapse if insufficient or immature bone occupies the suture gap. Therefore, we used H&E to determine the role of Pyk2 on the width, height, and area of the fibrous regions in control and expanded groups. After expansion, the width of the fibrous region was significantly increased in both mice genotypes ($p < 0.0001$) (Table 3, Fig. 12). The width of fibrous region in Pyk2-KO was significantly less than the width in WT mice in the 10 g and 20 g force groups ($p < 0.05$) (Table 2, Fig. 12). Although the width of fibrous region in the 10 g force groups was overall lower than the 20 g force groups, no significant difference in the width of the suture was observed between the 10 g and 20 g force groups for either the Pyk2-KO or WT mice (Table 3). The fibrous area in the middle of suture in the 10 g force group was significantly lower in Pyk2-KO mice compared to WT mice ($p < 0.05$) (Table 2, Fig. 14). However, the average height of the fibrous region was independent of treatment group or mouse genotype (Fig. 13).

Cartilage area and hypertrophic chondrocyte number are increased by suture expansion.

Secondary cartilages appear in the midpalatal suture of rodent animal and have the potential to ossify in the suture^[20, 44]. Therefore, to detect cartilage in our expanded sutures, we used alcian blue staining as shown in Figure 15. Alcian blue images demonstrated that a thin layer chondrocytes and cartilage covered the bony edges of the midpalatal suture in Pyk2-KO and WT control groups. After suture expansion, the pre-existing chondrocytes and cartilage were separated laterally, and numerous chondrocytes appeared in midpalatal sutures. We used image analysis software to quantitate the cartilage area and the number of hypertrophic chondrocytes which could be distinguished

morphologically based on their enlarged cell size and distinct nucleus. The cartilage area and the number of hypertrophic chondrocytes were significantly greater after expansion ($p < 0.0001$) (Table 3, Fig. 16, 17). There was no significant difference in cartilage area between the 10 g and 20 g force groups either in Pyk2-KO and WT mice, although the overall cartilage area in the 10 g force group was higher than the 20 g force group. Cartilage area and chondrocyte number were not significantly different between Pyk2-KO and WT mice (Table 2). Therefore, Pyk2-deficiency does not appear to affect the formation of secondary cartilage in the suture with or without expansion.

TABLES

Outcome	Force	Pyk2-KO Mean (SD)	WT Mean (SD)
BV/TV	0 g	90.81 (3.56)	84.10 (4.17)
	10 g	85.61 (4.95)	75.38 (6.99)
	20 g	80.55 (4.27)	65.89 (4.61)
Suture width	0 g	79.82 (7.97)	90.71 (13.32)
	10 g	341.06 (59.31)	476.79 (62.19)
	20 g	453.01 (66.61)	578.23 (63.50)
Maxilla width	0 g	2988.34 (101.18)	3062.63 (73.08)
	10 g	3418.67 (104.47)	3689.68 (138.91)
	20 g	3553.63 (150.78)	3745.46 (77.75)
Width of fibrous region	0 g	46.35 (2.97)	48.65 (9.59)
	10 g	326.81 (53.5)	441.5 (83.85)
	20 g	422.61 (95.45)	532.83 (67.05)
Height of fibrous region	0 g	NA	NA
	10 g	130.13 (29.91)	120.12 (37.38)
	20 g	116.54 (33.24)	100.09 (32.52)
Area of fibrous region	0 g	NA	NA
	10 g	45974.3 (3717.5)	57592.8 (9095)
	20 g	54658.3 (14962.3)	57057.7 (12974)
Oc.S/BS	0 g	0.072 (0.032)	0.074 (0.016)
	10 g	0.091 (0.019)	0.131 (0.022)
	20 g	0.096 (0.028)	0.172 (0.031)
Cartilage area	0 g	17162 (2901.7)	15533 (2799.6)
	10 g	105592 (20560.1)	97532 (32051.1)
	20 g	87220 (17553.1)	78126 (11614.8)
Hypertrophic chondrocyte number	0 g	30.5 (5.52)	28.08 (6.05)
	10 g	119.33 (31.99)	102.67 (22.06)
	20 g	100.89 (17.35)	95.67 (19.00)

TABLE 1. Summary of tissue parameters for control and expanded mice

The table shows the mean and standard deviation (SD) for all our data sets (NA; not applicable).

Outcome	Mouse Comparison	All	0 g	10 g	20 g
BV/TV	Pyk2-KO vs. WT	<0.0001	0.0134	0.0151	0.0002
Suture width	Pyk2-KO vs. WT	<0.0001	0.1166	0.0031	0.0076
Maxilla width	Pyk2-KO vs. WT	<0.0001	0.17746	0.0034	0.0198
Width of fibrous region	Pyk2-KO vs. WT	0.0018	0.5877	0.018	0.0432
Height of fibrous region	Pyk2-KO vs. WT	0.3316	NA	0.6197	0.4065
Area of fibrous region	Pyk2-KO vs. WT	0.0246	NA	0.001	0.5888
Oc.S/BS	Pyk2-KO vs. WT	0.0001	0.8588	0.0072	0.0011
Cartilage area	Pyk2-KO vs. WT	0.2874	0.3467	0.6154	0.3148
Hypertrophic chondrocyte number	Pyk2-KO vs. WT	0.2097	0.4866	0.3181	0.6299

TABLE 2. Statistical analysis of mouse comparison.

The table shows comparison between Pyk2-KO and WT mice among different expansion force levels. Highlighted boxes denote statistical significance ($p < 0.05$)

Outcome	Force Comparison	All	Pyk2-KO	WT
BV/TV	0 g vs. 10 g	0.002	0.0632	0.0254
	0 g vs. 20 g	<0.0001	0.0011	<0.0001
	10 g vs. 20 g	0.001	0.0873	0.0195
Suture width	0 g vs. 10 g	<0.0001	<0.0001	<0.0001
	0 g vs. 20 g	<0.0001	<0.0001	<0.0001
	10 g vs. 20 g	<0.0001	0.0117	0.0189
Maxilla width	0 g vs. 10 g	<0.0001	<0.0001	<0.0001
	0 g vs. 20 g	<0.0001	<0.0001	<0.0001
	10 g vs. 20 g	0.0528	0.1017	0.4108
Width of fibrous region	0 g vs. 10 g	<0.0001	<0.0001	<0.0001
	0 g vs. 20 g	<0.0001	<0.0001	<0.0001
	10 g vs. 20 g	0.0017	0.0576	0.0638
Height of fibrous region	0 g vs. 10 g	NA	NA	NA
	0 g vs. 20 g	NA	NA	NA
	10 g vs. 20 g	0.2206	0.4738	0.3454
Area of fibrous region	0 g vs. 10 g	NA	NA	NA
	0 g vs. 20 g	NA	NA	NA
	10 g vs. 20 g	0.1511	0.0639	0.9725
Oc.S/BS	0 g vs. 10 g	0.001	0.2269	0.0005
	0 g vs. 20 g	<0.0001	0.1857	<0.0001
	10 g vs. 20 g	0.032	0.7198	0.0233
Cartilage area	0 g vs. 10 g	<0.0001	<0.0001	<0.0001
	0 g vs. 20 g	<0.0001	<0.0001	<0.0001
	10 g vs. 20 g	0.012	0.127	0.1934
Hypertrophic chondrocyte number	0 g vs. 10 g	<0.0001	<0.0001	<0.0001
	0 g vs. 20 g	<0.0001	<0.0001	<0.0001
	10 g vs. 20 g	0.1105	0.2427	0.5689

TABLE 3. Statistical analysis of expansion force comparison.

The table shows comparison among expansion force levels either in Pyk2-KO or WT mice. Highlighted boxes denote statistical significance ($p < 0.05$)

FIGURES

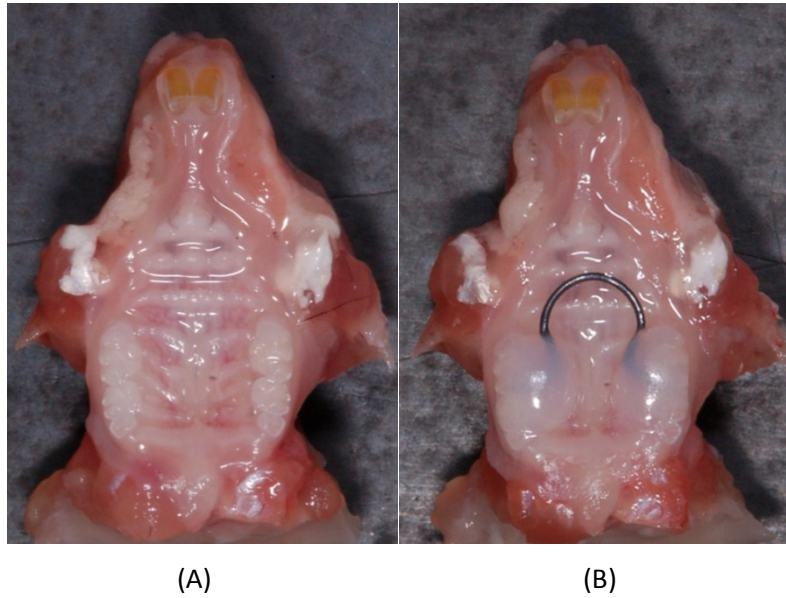


FIGURE 1. Occlusal view of midpalatal suture in 6-week-old mice.

(A) Maxilla without expander, non-treated control. (B) Experimental maxilla with a Ni-Ti expander bonded to first and second molars with resin.

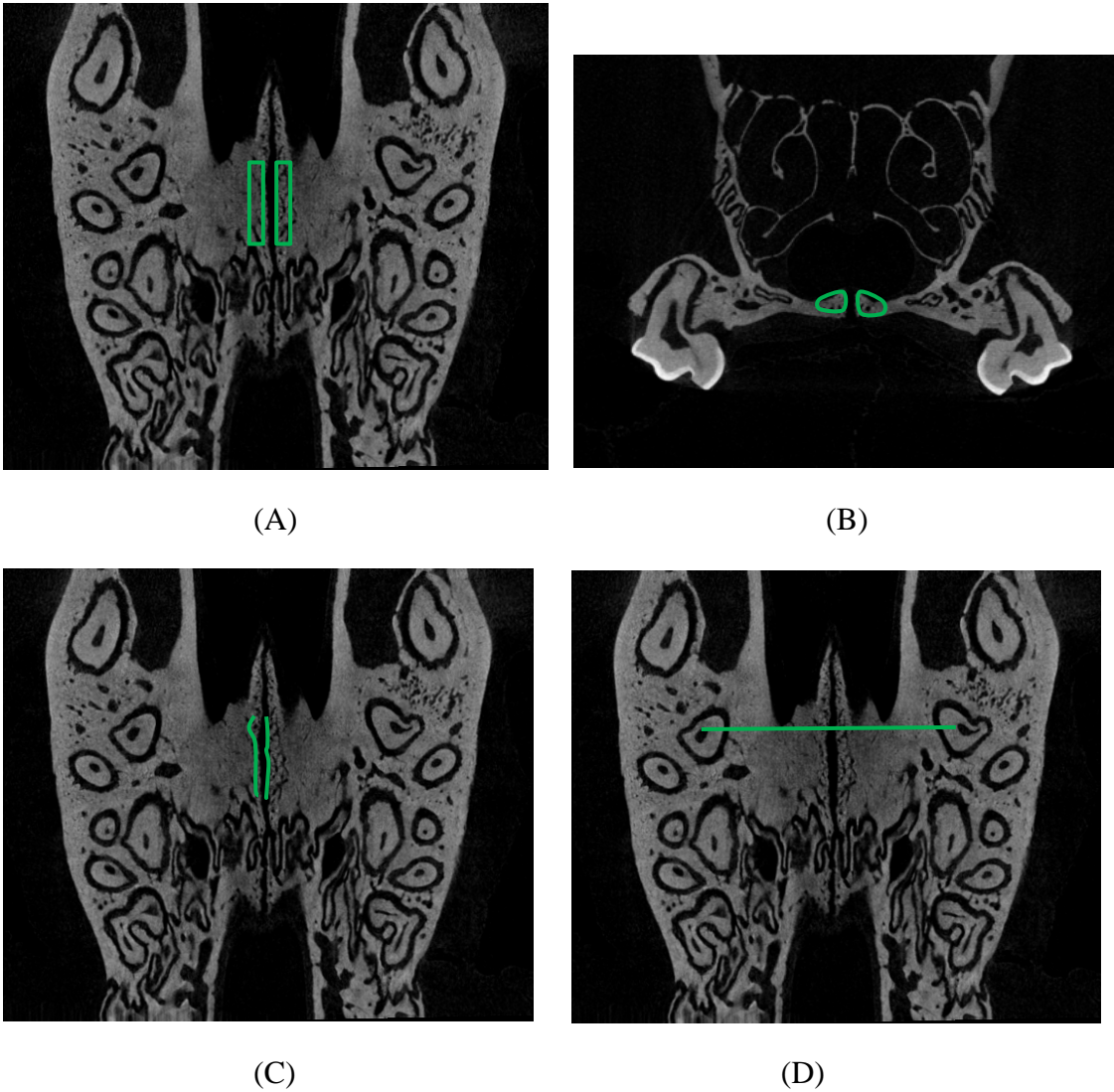


FIGURE 2. Micro-CT images for measurement.

(A) ROI on transverse plane (B) ROI on coronal plane (C) Suture width was measured by tracing two bony edges of the midpalatal suture. (D) Maxilla width was measured as the distance between canals of palatal roots of the right and left first molars. .

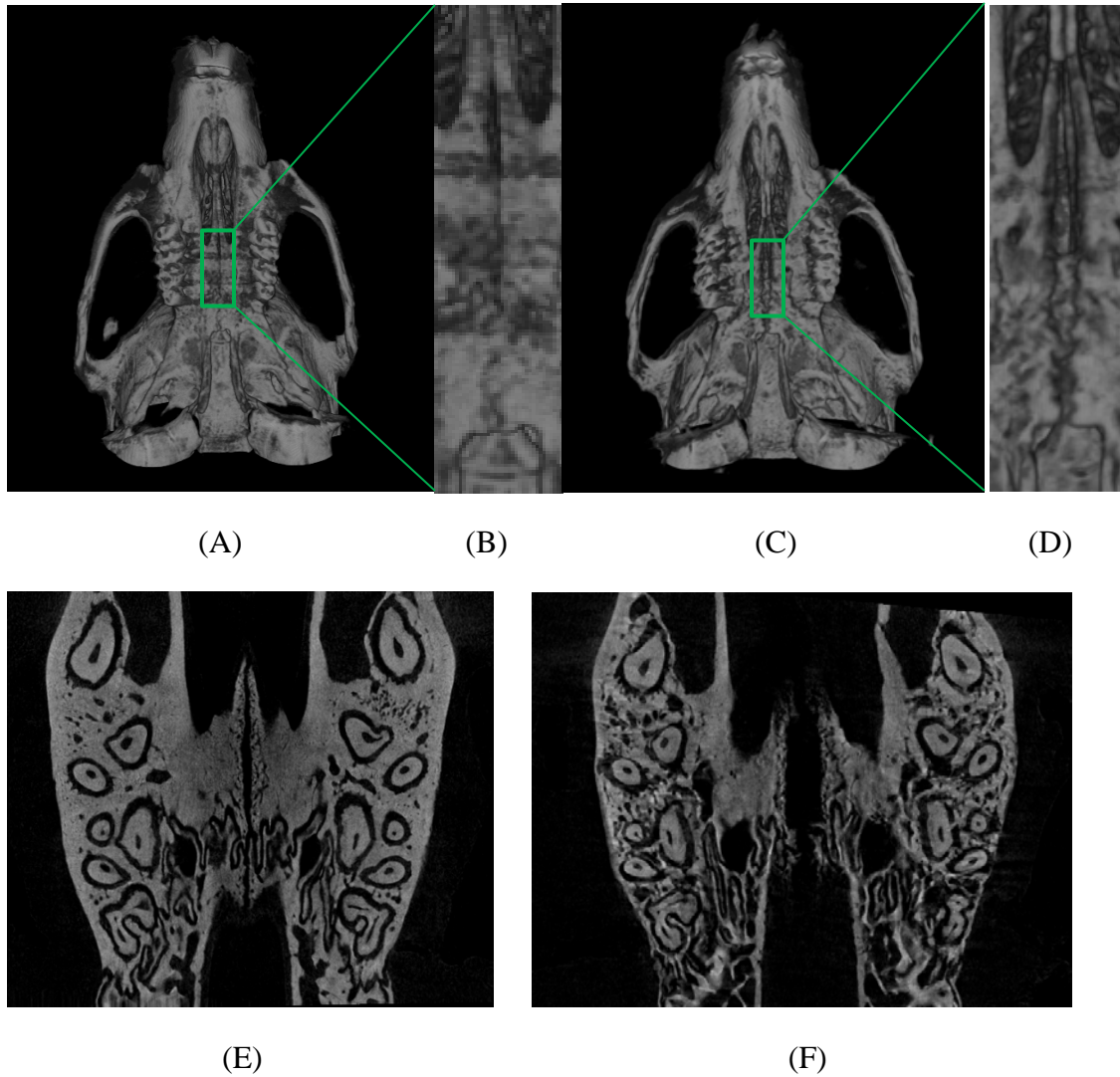


FIGURE 3. Three dimensional micro-CT reconstructed images of control and expanded sutures.

Occlusal view of reconstructed skull of control (A) and expanded (C) animals at day 14.

(B) and (D) are high magnification images of the areas marked by rectangles in panels (A)

and (C), respectively. (E) Transverse section of Pyk2-KO control mouse. (F)

Representative 3D image of transverse section of Pyk2-KO mouse subjected to 20 g expansion force.

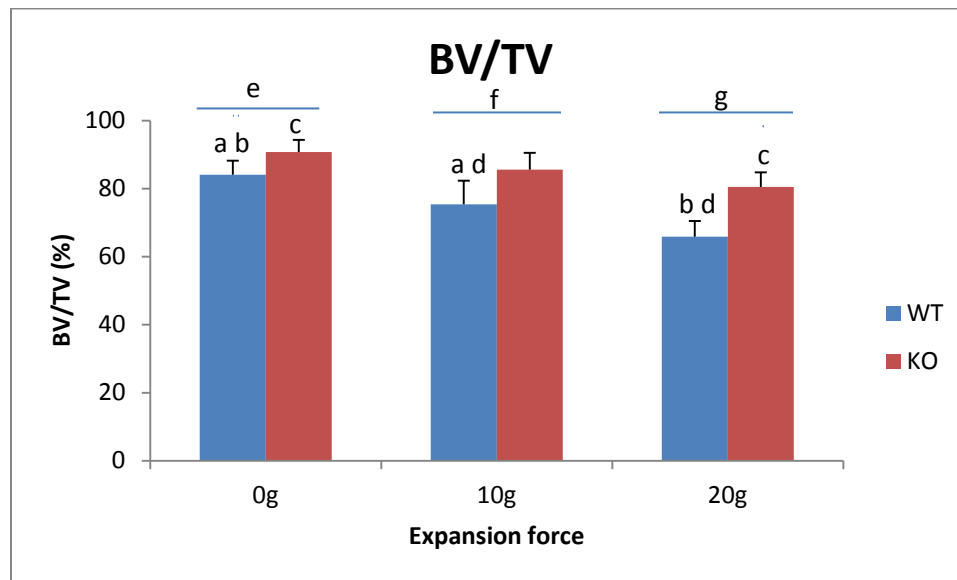


FIGURE 4. The ratio of BV/TV from micro-CT analysis.

Statistical analysis showed that the BV/TV was significantly higher in Pyk2-KO mice than the WT group among force levels ($p < 0.0001$). There was no significant difference between the control group (0 g) and 10 g expansion force groups in Pyk2-KO mice. The 20 g force induced the lowest BV/TV in both Pyk2-KO and WT mice ($p < 0.001$). The letters indicate statistically significant differences between groups at $p < 0.05$.

- a: 0 g versus 10 g force groups in WT mice
- b: 0 g versus 20 g force groups in WT mice
- c: 0 g versus 20 g force groups in Pyk2-KO mice
- d: 10 g versus 20 g force groups in WT mice
- e: WT versus Pyk2-KO for 0 g groups
- f: WT versus Pyk2-KO for 10 g force groups
- g: WT versus Pyk2-KO for 20 g force groups

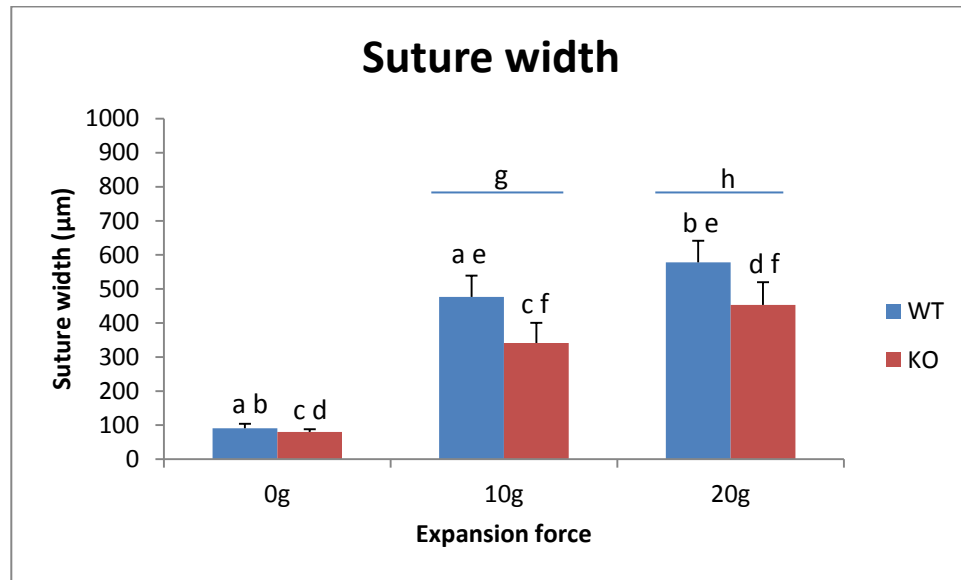


FIGURE 5. Suture width from micro-CT analysis.

The suture width in Pyk2-KO was significantly narrower than the width in WT mice after expansion ($p < 0.0001$). The width under 20 g expansion force was the significantly highest among force levels in both types of mice ($p < 0.0001$). The letters indicate statistically significant differences between groups at $p < 0.05$.

a: 0 g versus 10 g force groups in WT mice

b: 0 g versus 20 g force groups in WT mice

c: 0 g versus 10 g force groups in Pyk2-KO mice

d: 0 g versus 20 g force groups in Pyk2-KO mice

e: 10 g versus 20 g force groups in WT mice

f: 10 g versus 20 g force groups in Pyk2-KO mice

g: WT versus Pyk2-KO mice for 10 g force groups

h: WT versus Pyk2-KO mice for 20 g force groups

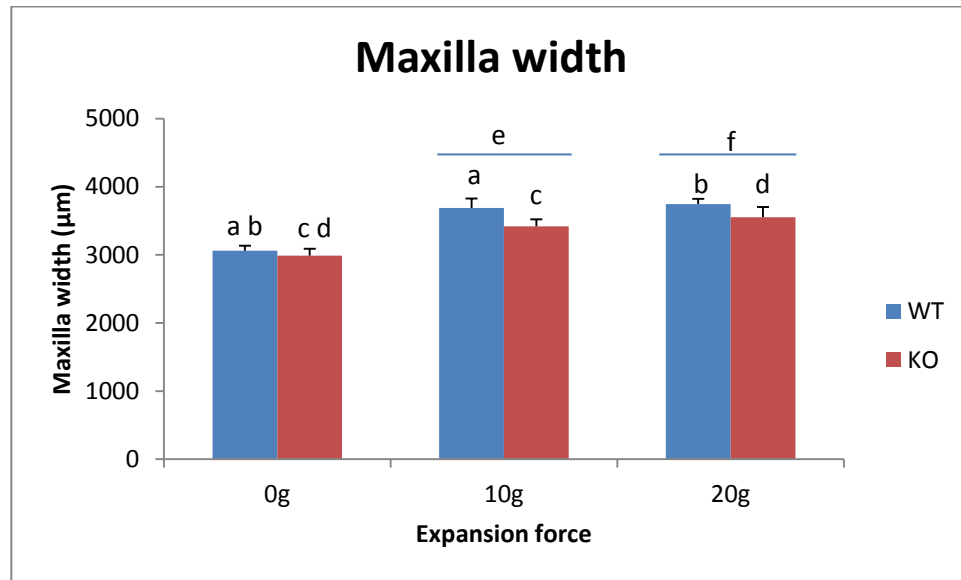


FIGURE 6. Maxilla width from micro-CT analysis.

The maxilla width in Pyk2-KO was significantly narrower than the width in WT mice after expansion ($p < 0.0001$), but no difference was shown between 10g and 20g force groups in both types of mice ($p > 0.05$). The letters indicate statistically significant differences between groups at $p < 0.05$.

a: 0 g versus 10 g force groups in WT mice

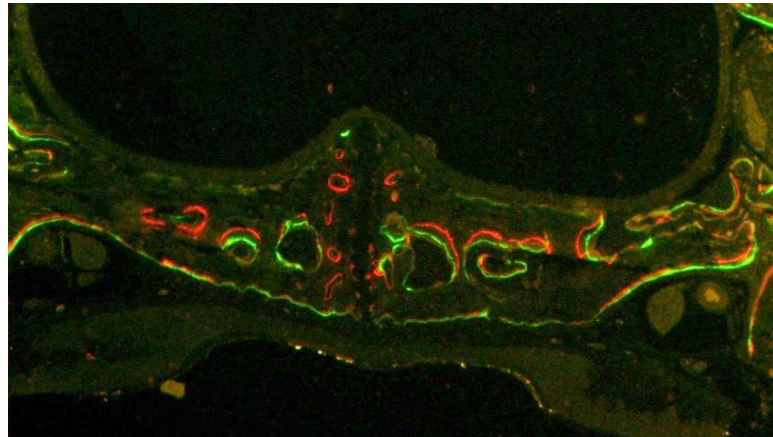
b: 0 g versus 20 g force groups in WT mice

c: 0 g versus 10 g force groups in Pyk2-KO mice

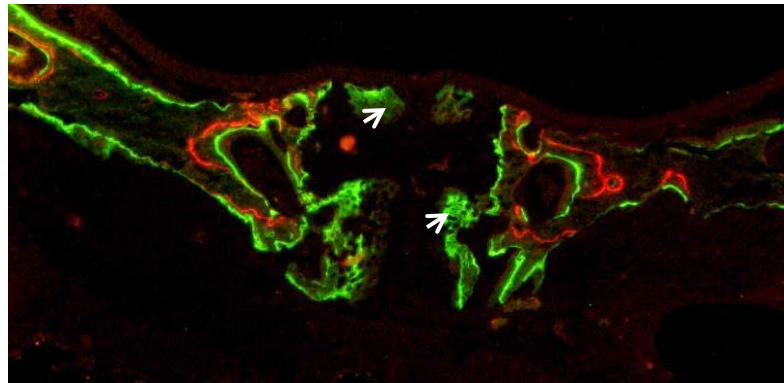
d: 0 g versus 20 g force groups in Pyk2-KO mice

e: WT versus Pyk2-KO mice for 10 g force groups

f: WT versus Pyk2-KO mice for 20 g force groups



(A)



(B)

FIGURE 7. Bone labeling of control and expanded midpalatal suture.

(A) Suture without expansion. (B) Expanded suture. Without expansion, the alizarin red and calcein green labels were difficult to observe along the bony edges of the suture. In the expanded suture, sharp calcein green labels were observed along the bone margins and diffused calcein green labels were observed on the oral and nasal sides of sutures where chondrocytes concentrated. However, alizarin red labels were too weak to be detected around the suture. White arrows (B) point to new bone formed in the expanded suture region after 14 days of expansion. The magnification of image is 40X.

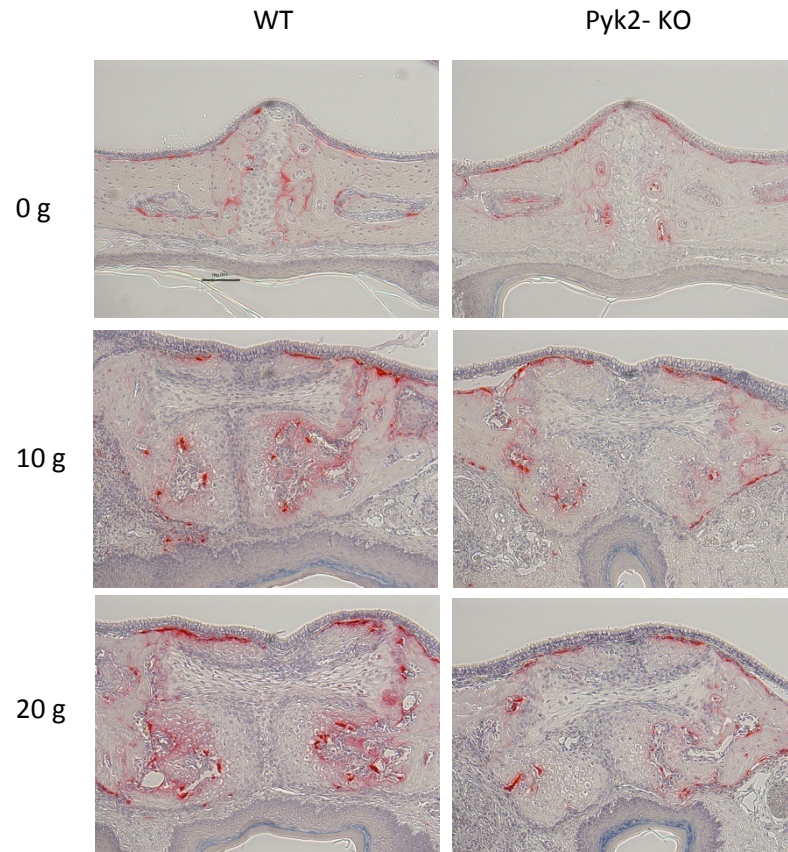


FIGURE 8. TRAP staining images of midpalatal suture.

TRAP-positive red cells were barely observed on TRAP staining sections in non-treated group either Pyk2-KO or WT mice. After expansion, the osteoclasts were obviously increased in midpalatal suture. The magnification of images is 100X. Scale bar: 100 μ m.

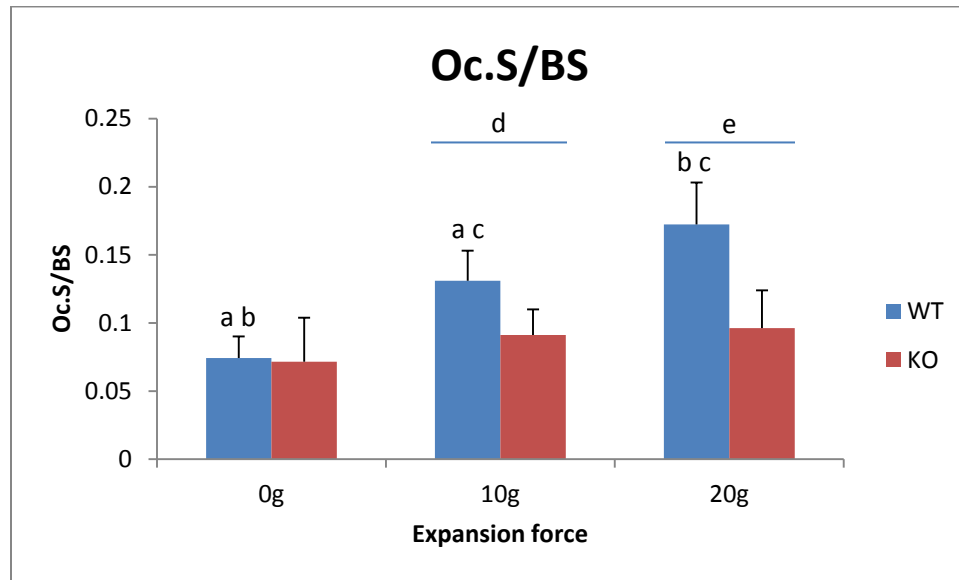


FIGURE 9. The ratio of Oc.S/ BS from TRAP staining.

Oc.S/BS in Pyk2-KO was significantly lower than WT mice in the 10 g and 20 g expansion force groups ($p < 0.05$). There was no significant difference among force levels in Pyk2-KO mice. The letters indicate statistically significant differences between groups at $p < 0.05$.

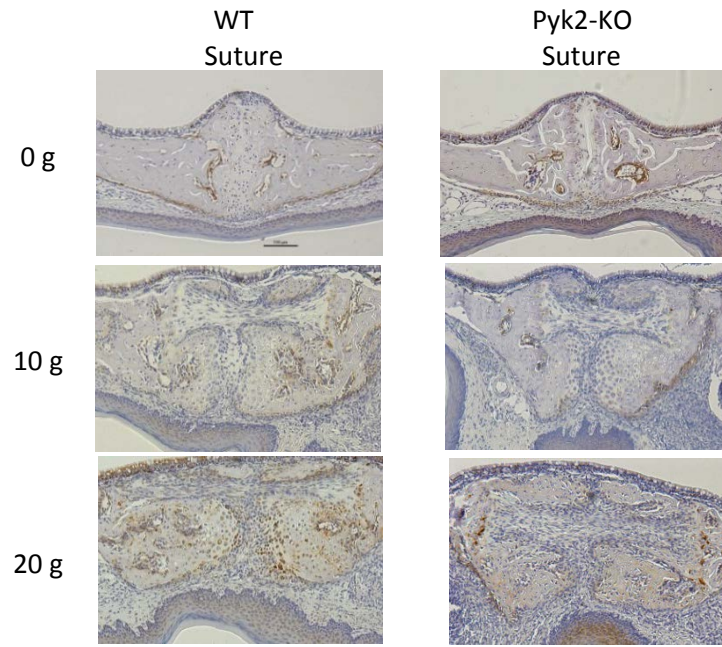
a: 0 g versus 10 g force groups in WT mice

b: 0 g versus 20 g force groups in WT mice

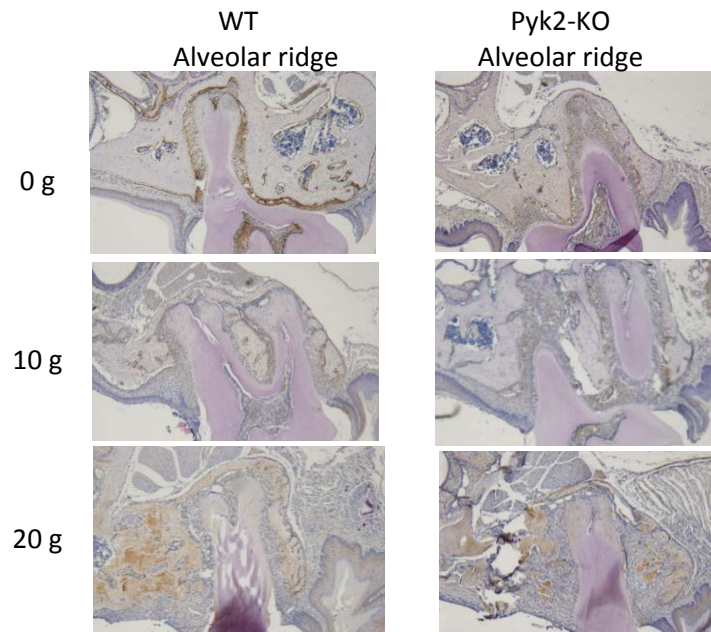
c: 10 g versus 20 g force groups in WT mice

d: WT versus Pyk2-KO mice for 10 g force groups

e: WT versus Pyk2-KO mice for 20 g force groups



(A)



(B)

FIGURE 10. ALP stained images of midpalatal suture and the alveolar ridge of molar.

(A) ALP expression in suture. (B) ALP expression in alveolar ridge. The brown signals were ALP positive cells. Alveolar ridge region was used as an internal labeling control. ALP expression appeared to be increased by expansion force in WT but not in Pyk2-KO mice. The magnification of image is 100X. Scale bar: 100 μ m

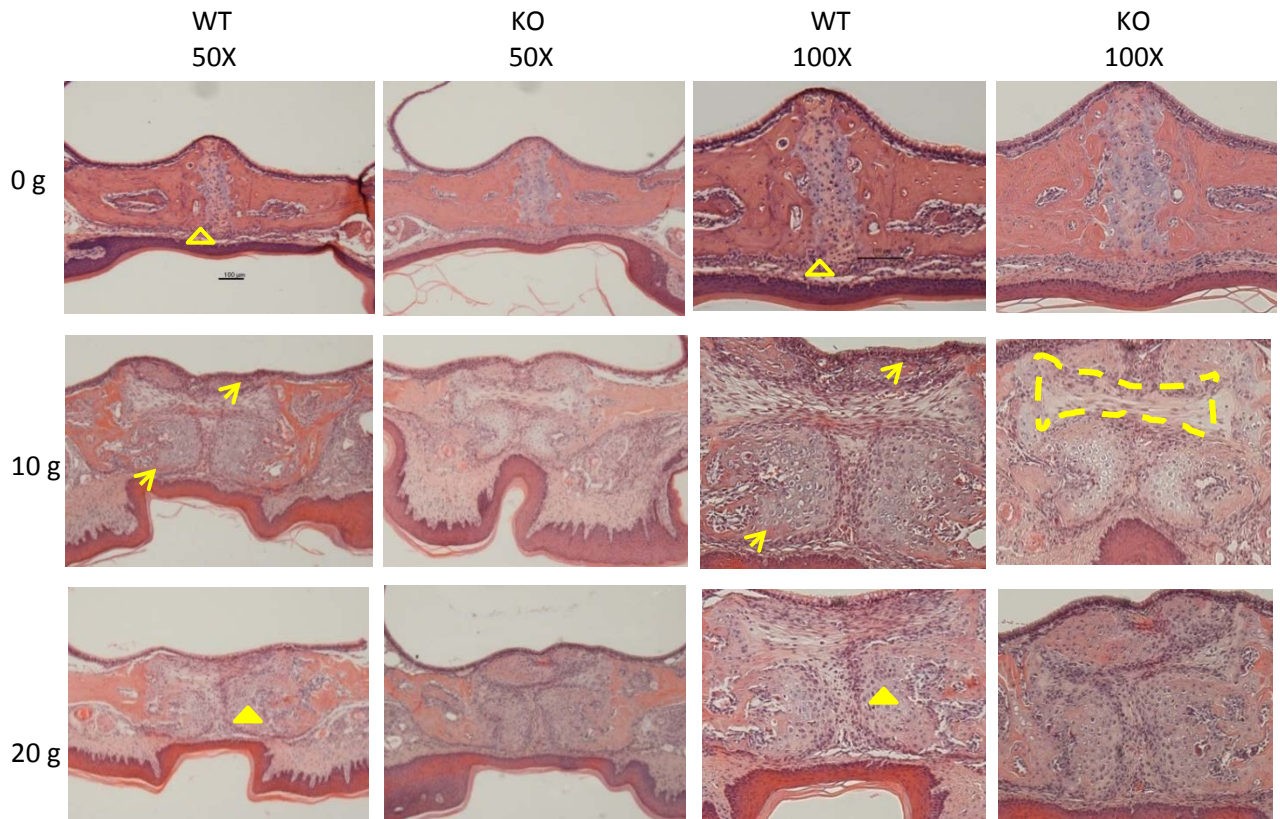


FIGURE 11. H&E stained images of the midpalatal suture.

After expansion, newly formed bone was observed adjacent to the periosteum on the oral side and was covered by chondrocytes along the suture margin. The open arrow head indicates the periosteum; closed arrowhead points to chondrocytes; arrows indicate new bone formed along the edge of palatal bones, and the dotted line defines the fibrous area surrounded by chondrocytes. Image magnifications are indicated. Scale bar: 100 μ m.

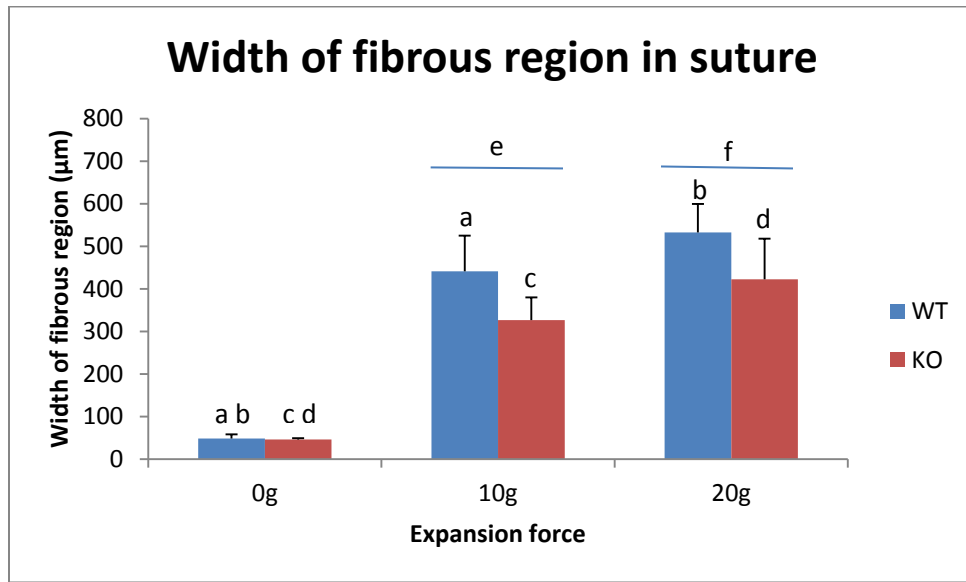


FIGURE 12. The width of fibrous region from H&E staining.

The fibrous region in WT was significantly wider than the fibrous region of Pyk2-KO mice in the 10 g and 20 g expansion force groups ($p < 0.05$). After expansion, the width of fibrous region was significantly increased in Pyk2-KO and WT mice ($p < 0.0001$). The letters indicate statistically significant differences between groups at $p < 0.05$.

a: 0 g versus 10 g force groups in WT mice

b: 0 g versus 20 g force groups in WT mice

c: 0 g versus 10 g force groups in Pyk2-KO mice

d: 0 g versus 20 g force groups in Pyk2-KO mice

e: WT versus Pyk2-KO mice for 10 g force groups

f: WT versus Pyk2-KO mice for 20 g force groups

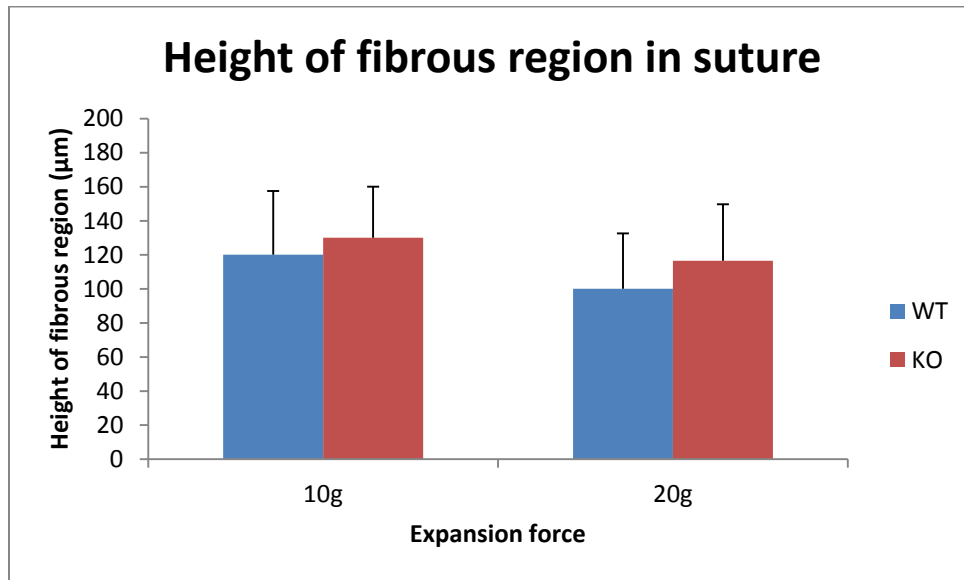


FIGURE 13. The height of fibrous region from H&E staining.

Statistical results indicated that the height of fibrous region was independent of the force levels and mouse genotypes ($p > 0.05$).

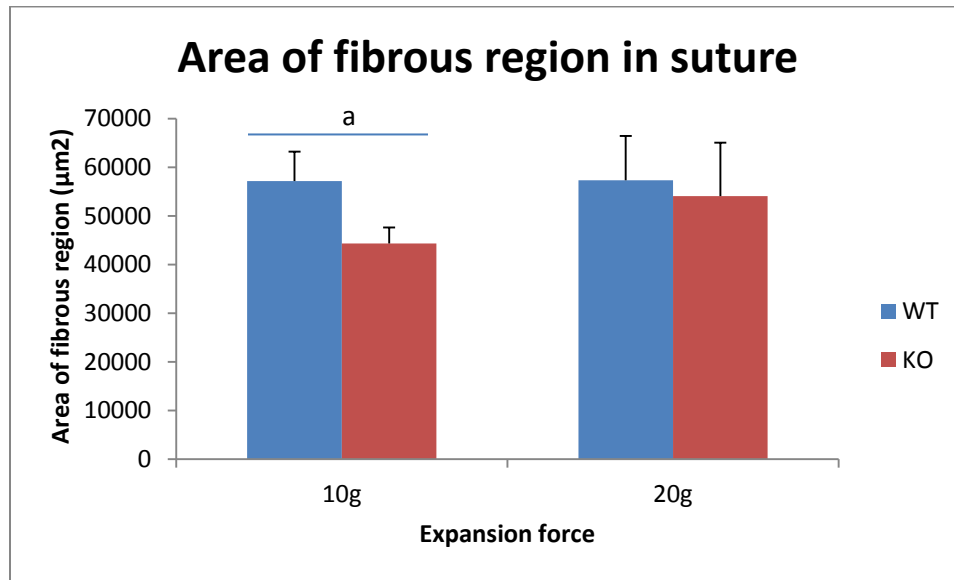


FIGURE 14. The area of fibrous region from H&E staining.

Statistical analysis showed that the area of fibrous region in the 10 g expansion force group of Pyk2-KO mice was significantly less than WT mice of same force group ($p < 0.05$). No difference was found between the 10 g and 20 g ($P > 0.05$). “a” indicates statistically significant differences at $p < 0.05$ between WT and Pyk2-KO in the 10 g expansion force group.

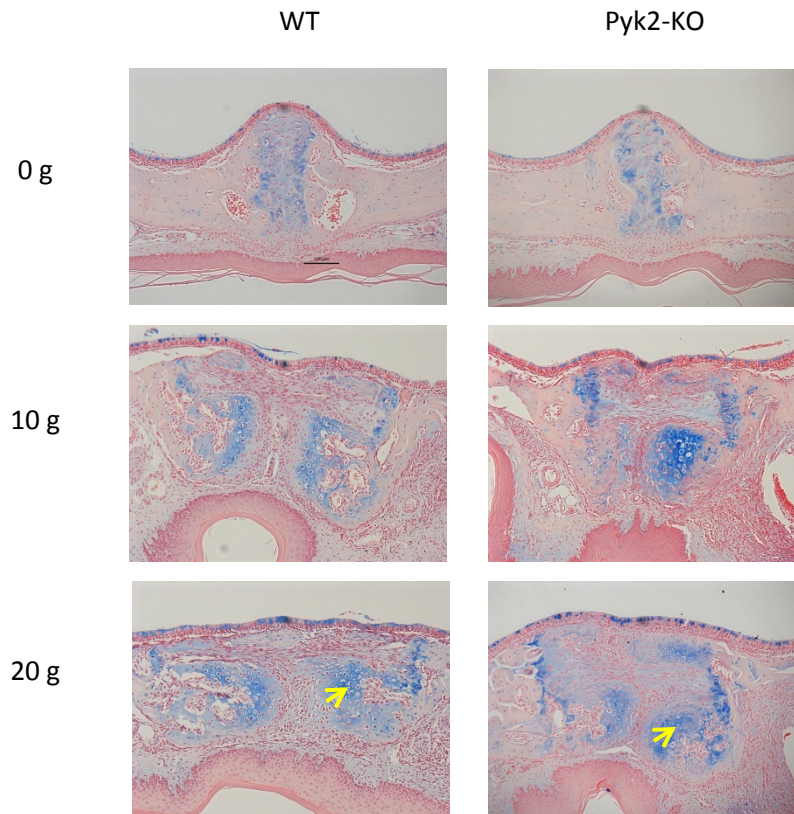


FIGURE 15. Alcian Blue staining of cartilage and chondrocytes.

The cartilage and chondrocytes, which are stained blue, appear to be significantly increased after expansion. The yellow arrows point to the hypertrophic chondrocytes which appear large and round. The magnification of image is 100X. Scale bar: 100 μ m.

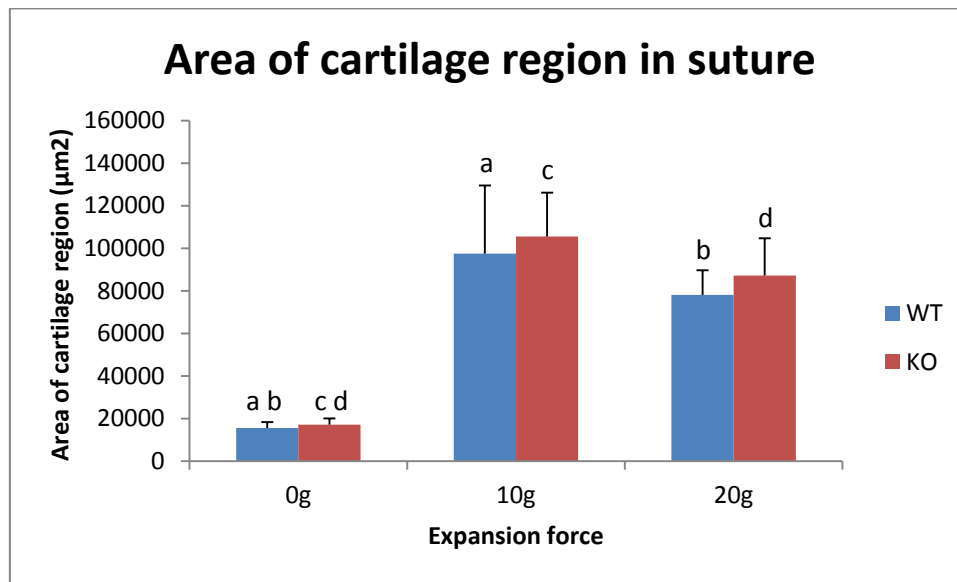


FIGURE 16. The area of cartilage region in sutures.

After expansion, the cartilage area was significantly increased in Pyk2-KO and WT mice ($p < 0.0001$). There was no significant difference in the cartilage area between genotypes among force levels ($p > 0.05$). The letters indicate statistically significant differences between groups at $p < 0.05$.

- a: 0 g versus 10 g force groups in WT mice
- b: 0 g versus 20 g force groups in WT mice
- c: 0 g versus 10 g force groups in Pyk2-KO mice
- d: 0 g versus 20 g force groups in Pyk2-KO mice

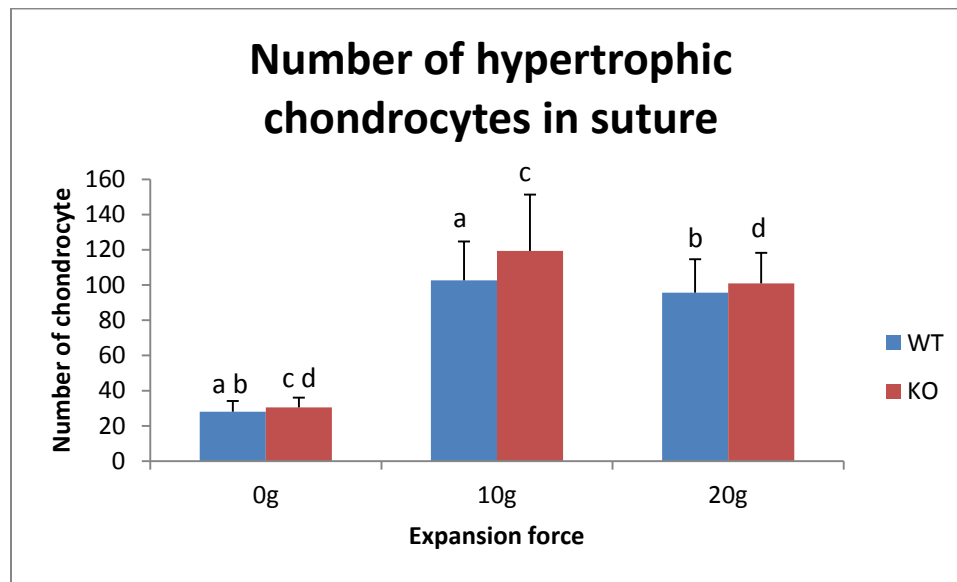


FIGURE 17. Hypertrophic chondrocytes number.

No significant difference the hypertrophic chondrocytes number was observed between Pyk2-KO and WT mice ($p > 0.05$). The number was obviously increased after expansion ($p < 0.0001$) but no difference between 10 g and 20 g force groups in both genotypes of mice ($p > 0.05$). The letters indicate statistically significant differences between groups at $p < 0.05$.

a: 0 g versus 10 g force groups in WT mice

b: 0 g versus 20 g force groups in WT mice

c: 0 g versus 10 g force groups in Pyk2-KO mice

d: 0 g versus 20 g force groups in Pyk2-KO mice

DISCUSSION

In the current study we examined whether Pyk2 plays a role in suture expansion and if a pharmaceutical agent to inhibit Pyk2 can be used to accelerate new bone formation at the suture margins in the expanded maxilla. We used Pyk2-KO and WT mice to investigate bone mass and remodeling of the midpalatal suture under two expansion forces, 10 g and 20 g. Control mice received no springs (0 g). Our data demonstrated both the 10 g and 20 g expansion forces resulted in maxilla expansion in Pyk2-KO and WT mice. However, Pyk2-KO mice had higher bone mass in the suture which was correlated with a narrow suture width. This suggests that Pyk2-deficiency leads to a smaller gap between the two palatal shelves with more dense bone, implying a more stable environment with a lower likelihood of treatment relapse.

Pyk2 mediates signaling pathways involved with the process of bone remodeling by acting on both osteoclasts and osteoblasts. Pyk2 deficiency impedes osteoclast activities, leading to decreases in osteoclast-mediated bone resorption. In the non-treated control groups, Pyk2-KO mice had a higher BV/TV ratio and similar Oc.S/BS compared to WT mice. In our study, TRAP images showed that more osteoclasts concentrated in the bone marrow around sutures in the WT expansion groups, indicating more osteoclasts engaged in bone resorption in WT mice. Therefore, the higher bone density of Pyk2-KO mice may result from the impairment of osteoclast function, which is consistent with previous studies^[29]. However, whether the expansion forces decreased osteoclast differentiation or increased apoptosis in Pyk2-KO mice is currently unknown.

During suture expansion, new bone forms at the suture margins, which is usually immature woven bone^[3,7]. In humans, it requires more than 3 months for new bone to remodel and become calcified after RME. Although this time frame is reduced in mice,

the decreases in BV/TV found in both Pyk2-KO and WT expansion groups compared to the genotype-matched control (0 g) groups, suggest that newly formed bone was not completely remodeled to become organized lamellar bone, leading to lower bone density. In future studies, increasing the retention time may allow for more bone remodeling and a higher final BV/TV in both WT and Pyk2-KO mice. Furthermore, it will be of interest to determine the role of Pyk2 on suture stability and decreasing relapse rate by removing springs after suture expansion and allowing mice to recover prior to necropsy.

RME initiates fibroblast proliferation and mesenchymal stem cell differentiation within several hours. The maxilla width, suture width and fibrous area were significantly increased in both genotypes of mice subjected to expansion forces. The stretched fibers filled in the central area of the sutures. The application of 20 g force on WT mice resulted in the widest suture gap, with higher number of osteoclasts, and a lower BV/TV than the 10 g force groups. These findings indicate mice that received the 20 g expander may have a higher potential for midpalatal suture relapse than the lower 10 g force groups. In addition, since Pyk2-KO mice exhibited higher BV/TV as well as a narrower suture width, our findings suggest that the expanded suture in Pyk2-KO mice may be more stable and more resistant to relapse than WT mice treated with the 10 g or 20 g forces.

To quantify bone formation in the suture following expansion, alizarin complexone and calcein fluorescent dyes were administered to Pyk2-KO and WT mice. The fluorescent labels can be bound to calcium ions and indicate the sites of mineralization, including the site of bone formation. Ten et al. ^[4] demonstrated that the new bone was formed by the pre-existing and undamaged osteoblasts within 3 to 4 days after expansion force application in rats. In addition to bone formation rate, the interlabel distance is

affected by the label clearance and calcium affinity. Alizarin complexone and calcein have shorter plasma half-lives than tetracycline. Calcein has higher calcium affinity compared to alizarin. The longer time intervals will increase the chances for label escape, whereas the shorter time intervals will make discrimination between the labels more difficult ^[45]. In the present study, the alizarin complexone was injected on day 1, when new bone may not have been formed and not yet deposited along the suture edges, although the strong red labels were observed around the bone marrow adjacent the suture in the palatine bone. On the other hand, the high bone turnover rate under expansion forces in the midpalatal suture may have caused significant bone resorption and the loss of the alizarin labels. Buckbinder et al. ^[30] demonstrated an increase in bone formation rate in the long bone of 18 week Pyk2-KO mice. Therefore, in future studies, decreasing the time interval between injection fluorescent dyes, or using multiple injections may enable bone formation rate determination in the suture. In addition, it may be necessary to examine bone formation rate at different expansion times.

ALP is an important marker of osteoblast maturation. Osteoblast differentiation is a multistep process associated with cell proliferation, matrix synthesis and matrix mineralization ^[46, 47]. The matrix maturation phase is characterized by maximal expression of ALP, whereas peak levels of expression of osteocalcin and osteopontin are achieved during matrix mineralization. In this study, qualitative assessment of ALP stained sections indicated that ALP expression appears to be increased by expansion forces in WT mice after 14 days expansion, although we were unable to quantify changes in Ob.S/BS (osteoblast surface per bone surface) due to technical issues related to our ALP staining. In future studies, it may be necessary to select an alternate bone marker

and/or include a series of expansion periods to detect the osteoblast activity status in the sutures of mice. Our studies revealed decreased Oc.S/BS in midpalatal sutures in Pyk2-KO mice. Since osteoclast number is controlled by the RANKL/OPG ratio secreted by osteoblasts, it is possible that expansion may have resulted in a local decrease in RANKL or an increase in OPG, or both in Pyk2-KO mice. However, the mechanism of interaction between osteoblasts and osteoclasts in Pyk2-KO mice during suture expansion remains to be determined.

Mechanical force can enhance the differentiation of mesenchymal cells into chondroprogenitor cells which produce secondary cartilage^[19]. Hypertrophic chondrocytes are terminal stage of differentiation in the chondrogenic cell lineage^[48]. These cells have unique phenotypic traits that relate to cartilage calcification and endochondral ossification. In our study, chondrocytes and secondary cartilage was found along the bone edges of suture of mice. After expansion, cartilage areas were significantly increased in WT and Pyk2-KO mice. Moreover, the 10 g expansion force induced more cartilage area compared to the 20 g force group. Numerous hypertrophic chondrocytes concentrated around the front of bone edges were also observed in expanded animal. However, no differences in the hypertrophic chondrocyte number or cartilage area were found between Pyk2-KO and WT mice. Similar to our findings, Liu et al.^[23] also reported that a 10 g expansion force induced a more preferable suture cartilage response pattern than a 20 g force.

The ossification pattern during RME of the suture is still unclear and may involve both intramembranous and endochondral bone formation. It has been reported that 56 g tensional forces applied to midpalatal sutures of mice induce bone formation in the

periosteum, which contains osteogenic progenitor cells, suggesting intramembranous ossification ^[14]. In contrast, Takahashi et al. ^[44] demonstrated that 10-20 g expansion forces induce cellular transition from cartilaginous tissue to bone in rat midpalatal sutures. Kobayashi et al. ^[20] also suggested that mesenchymal cells located on the inner side of the cartilaginous tissue can proliferate and differentiate into osteoblasts in rats under midpalatal suture expansion. These latter studies suggest the occurrence of endochondral ossification in the suture. In our studies, histological staining with H&E on tissue sections after force-induced expansion revealed the presence of newly formed bone adjacent to the periosteum of the palatine bone. We also found that the suture margins were covered by chondrocytes. In addition, diffused green fluorescence labels (calcein) in the same region of the sutures where chondrocytes were concentrated. Therefore, we cannot exclude the possibility of endochondral bone formation in the suture.

SUMMARY AND CONCLUSIONS

As mentioned previously, the null hypothesis, that there would be no difference of bone mass in the midpalatal suture between Pyk2-KO mice and WT mice following suture expansion, was rejected. Our findings supported the alternate hypothesis. We found the following:

1. After suture expansion, increased bone marrow spaces appeared around suture edges; BV/TV was significantly reduced.
2. After suture expansion, the suture width, fibrous area in the middle zone of suture, osteoclast number, cartilage area and hypertrophic chondrocyte number were all significantly increased.
3. The suture BV/TV in Pyk2-KO mice was significantly higher than in WT mice. Moreover, Pyk2-KO exhibited reduced suture width, maxilla width, fibrous area, and osteoclast number per bone surface (Oc.S/BS) compared to WT mice under expansion forces.
4. Cartilage area and hypertrophic chondrocyte number were independent of mouse genotypes.

In conclusion, Pyk2-deficiency increased the bone mass and decreased the suture width following expansion, while still allowing expansion of the maxilla. Therefore, our data suggest that suture expansion in Pyk2-KO may result in a more stable which is more resistant to relapse than WT mice. Furthermore, our studies suggest that therapeutic approaches to inhibit Pyk2 in the suture may increase bone mass to reduce relapse of the arch width following mechanical expansion.

REFERENCES

1. Kumar, S.A., Gurunathan, D., and Muruganandham, S.S., *Rapid Maxillary Expansion: A Unique Treatment Modality in Dentistry*. J Clin Diagn Res, 2011. 5(4): p. 906-911.
2. Wertz, R.A., *Skeletal and dental changes accompanying rapid midpalatal suture opening*. American journal of orthodontics, 1970. 58(1): p. 41-66.
3. Wagemans, P.A., van de Velde, J.-P., and Kuljpers-Jagtman, A.M., *Sutures-and forces: A review*. American Journal of Orthodontics and Dentofacial Orthopedics, 1988. 94(2): p. 129-141.
4. Ten Cate, A., Freeman, E., and Dickinson, J., *Sutural development: structure and its response to rapid expansion*. American journal of orthodontics, 1977. 71(6): p. 622-636.
5. Johnson, B.M., McNamara Jr, J.A., Bandeen, R.L., and Baccetti, T., *Changes in soft tissue nasal widths associated with rapid maxillary expansion in prepubertal and postpubertal subjects*. The Angle Orthodontist, 2010. 80(6): p. 995-1001.
6. Franchi, L., Baccetti, T., Lione, R., Fanucci, E., and Cozza, P., *Modifications of midpalatal sutural density induced by rapid maxillary expansion: a low-dose computed-tomography evaluation*. American Journal of Orthodontics and Dentofacial Orthopedics, 2010. 137(4): p. 486-488.
7. Cleall, J.F., Bayne, D.I., Posen, J.M., and Subtelny, J.D., *Expansion of the midpalatal suture in the monkey*. The Angle orthodontist, 1965. 35(1): p. 23-35.
8. Liu, S.S.-Y., Xu, H., Sun, J., Kontogiorgos, E., Whittington, P.R., Misner, K.G., Kyung, H.-M., Buschang, P.H., and Opperman, L.A., *Recombinant human bone morphogenetic protein-2 stimulates bone formation during interfrontal suture expansion in rabbits*. American Journal of Orthodontics and Dentofacial Orthopedics, 2013. 144(2): p. 210-217.
9. Storey, E., *Tissue response to the movement of bones*. American journal of orthodontics, 1973. 64(3): p. 229-247.
10. Herring, S., *Mechanical influences on suture development and patency*. 2008.
11. Takahashi, I., Onodera, K., Sasano, Y., Mizoguchi, I., Bae, J.-W., Mitani, H., Kagayama, M., and Mitani, H., *Effect of stretching on gene expression of $\beta 1$ integrin and focal adhesion kinase and on chondrogenesis through cell-extracellular matrix interactions*. European journal of cell biology, 2003. 82(4): p. 182-192.
12. Mao, J.J. and Nah, H.-D., *Growth and development: hereditary and mechanical modulations*. American Journal of Orthodontics and Dentofacial Orthopedics, 2004. 125(6): p. 676-689.
13. Decker, J.D. and Hall, S.H., *Light and electron microscopy of the new born sagittal suture*. The Anatomical Record, 1985. 212(1): p. 81-89.
14. Hou, B., Fukai, N., and Olsen, B.R., *Mechanical force-induced midpalatal suture remodeling in mice*. Bone, 2007. 40(6): p. 1483-1493.
15. Mao, J.J., Wang, X., and Kopher, R.A., *Biomechanics of craniofacial sutures: orthopedic implications*. The Angle Orthodontist, 2003. 73(2): p. 128-135.
16. Katebi, N., Kolpakova - Hart, E., Lin, C., and Olsen, B., *The mouse palate and its cellular responses to midpalatal suture expansion forces*. Orthodontics & craniofacial research, 2012. 15(3): p. 148-158.
17. Pritchard, J., Scott, J., and Girgis, F.G., *The structure and development of cranial and facial sutures*. Journal of anatomy, 1956. 90(Pt 1): p. 73.
18. Forbes, D. and Al-Bareedi, S., *Inhibition of secondary cartilage of the intermaxillary suture in Sprague-Dawley rats following the enucleation of maxillary molars*. Journal of craniofacial genetics and developmental biology, 1985. 6(1): p. 73-88.

19. Hall, B., *Selective proliferation and accumulation of chondroprogenitor cells as the mode of action of biomechanical factors during secondary chondrogenesis*. Teratology, 1979. 20(1): p. 81-91.
20. Kobayashi, E., Hashimoto, F., Kobayashi, Y., Sakai, E., Miyazaki, Y., Kamiya, T., Kobayashi, K., Kato, Y., and Sakai, H., *Force-induced rapid changes in cell fate at midpalatal suture cartilage of growing rats*. Journal of dental research, 1999. 78(9): p. 1495-1504.
21. Boyce, B.F. and Xing, L., *Functions of RANKL/RANK/OPG in bone modeling and remodeling*. Archives of biochemistry and biophysics, 2008. 473(2): p. 139-146.
22. Burr, D.B. and Allen, M.R., *Basic and applied bone biology*. 2013: Academic Press.
23. Liu, Y., Tang, Y., Xiao, L., Liu, S.S.-Y., and Yu, H., *Suture cartilage formation pattern varies with different expansive forces*. American Journal of Orthodontics and Dentofacial Orthopedics, 2014. 146(4): p. 442-450.
24. Luo, T., Zhang, W., Shi, B., Cheng, X., and Zhang, Y., *Enhanced bone regeneration around dental implant with bone morphogenetic protein 2 gene and vascular endothelial growth factor protein delivery*. Clinical oral implants research, 2012. 23(4): p. 467-473.
25. Lai, R.-F., Zhou, Z.-Y., and Chen, T., *Accelerating bone generation and bone mineralization in the interparietal sutures of rats using an rhBMP-2/ACS composite after rapid expansion*. Experimental Animals, 2013. 62(3): p. 189.
26. Lee, K., Sugiyama, H., Imoto, S., and Tanne, K., *Effects of bisphosphonate on the remodeling of rat sagittal suture after rapid expansion*. The Angle orthodontist, 2001. 71(4): p. 265-273.
27. Fu, R., Selph, S., McDonagh, M., Peterson, K., Tiwari, A., Chou, R., and Helfand, M., *Effectiveness and harms of recombinant human bone morphogenetic protein-2 in spine fusion: a systematic review and meta-analysis*. Annals of internal medicine, 2013. 158(12): p. 890-902.
28. Migliorati, C.A., *Bisphosphonates and oral cavity avascular bone necrosis*. Journal of Clinical Oncology, 2003. 21(22): p. 4253-4254.
29. Gil-Henn, H., Destaing, O., Sims, N.A., Aoki, K., Alles, N., Neff, L., Sanjay, A., Bruzzaniti, A., De Camilli, P., and Baron, R., *Defective microtubule-dependent podosome organization in osteoclasts leads to increased bone density in Pyk2^{-/-} mice*. The Journal of cell biology, 2007. 178(6): p. 1053-1064.
30. Buckbinder, L., Crawford, D.T., Qi, H., Ke, H.Z., Olson, L.M., Long, K.R., Bonnette, P.C., Baumann, A.P., Hambor, J.E., and Grasser, W.A., *Proline-rich tyrosine kinase 2 regulates osteoprogenitor cells and bone formation, and offers an anabolic treatment approach for osteoporosis*. Proceedings of the National Academy of Sciences, 2007. 104(25): p. 10619-10624.
31. Duong, L.T., Lakkakorpi, P.T., Nakamura, I., Machwate, M., Nagy, R.M., and Rodan, G.A., *PYK2 in osteoclasts is an adhesion kinase, localized in the sealing zone, activated by ligation of alpha (v) beta3 integrin, and phosphorylated by src kinase*. Journal of Clinical Investigation, 1998. 102(5): p. 881.
32. Okigaki, M., Davis, C., Falasca, M., Harroch, S., Felsenfeld, D., Sheetz, M., and Schlessinger, J., *Pyk2 regulates multiple signaling events crucial for macrophage morphology and migration*. Proceedings of the National Academy of Sciences, 2003. 100(19): p. 10740-10745.
33. Duong, L.T., Nakamura, I., Lakkakorpi, P.T., Lipfert, L., Bett, A.J., and Rodan, G.A., *Inhibition of osteoclast function by adenovirus expressing antisense protein-tyrosine kinase 2*. Journal of Biological Chemistry, 2001. 276(10): p. 7484-7492.

34. Stein, G.S. and Lian, J.B., *Molecular mechanisms mediating developmental and hormone-regulated expression of genes in osteoblasts*, in *Cellular and molecular biology of bone*. 1993, Academic Press San Diego. p. 48-95.
35. Kasperk, C., Wergedal, J., Strong, D., Farley, J., Wangerin, K., Gropp, H., Ziegler, R., and Baylink, D.J., *Human bone cell phenotypes differ depending on their skeletal site of origin*. *The Journal of Clinical Endocrinology & Metabolism*, 1995. 80(8): p. 2511-2517.
36. Young, S., Hum, J.M., Rodenberg, E., Turner, C.H., and Pavalko, F.M., *Non-overlapping functions for Pyk2 and FAK in osteoblasts during fluid shear stress-induced mechanotransduction*. *PloS one*, 2011. 6(1): p. e16026.
37. Loeser, R.F., Forsyth, C.B., Samarel, A.M., and Im, H.-J., *Fibronectin fragment activation of proline-rich tyrosine kinase PYK2 mediates integrin signals regulating collagenase-3 expression by human chondrocytes through a protein kinase C-dependent pathway*. *Journal of Biological Chemistry*, 2003. 278(27): p. 24577-24585.
38. Ding, L., Guo, D., and Homandberg, G., *Fibronectin fragments mediate matrix metalloproteinase upregulation and cartilage damage through proline rich tyrosine kinase 2, c-src, NF- κ B and protein kinase C δ* . *Osteoarthritis and cartilage*, 2009. 17(10): p. 1385-1392.
39. Whitney, N.P., Lamb, A.C., Louw, T.M., and Subramanian, A., *Integrin-mediated mechanotransduction pathway of low-intensity continuous ultrasound in human chondrocytes*. *Ultrasound in medicine & biology*, 2012. 38(10): p. 1734-1743.
40. Jang, K.W., Ding, L., Seol, D., Lim, T.-H., Buckwalter, J.A., and Martin, J.A., *Low-intensity pulsed ultrasound promotes chondrogenic progenitor cell migration via focal adhesion kinase pathway*. *Ultrasound in medicine & biology*, 2014. 40(6): p. 1177-1186.
41. Thompson, S., *An overview of nickel–titanium alloys used in dentistry*. *International Endodontic Journal*, 2000. 33(4): p. 297-310.
42. Erlebacher, A. and Derynck, R., *Increased expression of TGF-beta 2 in osteoblasts results in an osteoporosis-like phenotype*. *The Journal of cell biology*, 1996. 132(1): p. 195-210.
43. Sheehan, D.C. and Hrapchak, B.B., *Theory and practice of histotechnology*. 1980: Cv Mosby.
44. Takahashi, I., Mizoguchi, I., Nakamura, M., Sasano, Y., Saitoh, S., Kagayama, M., and Mitani, H., *Effects of expansive force on the differentiation of midpalatal suture cartilage in rats*. *Bone*, 1996. 18(4): p. 341-348.
45. van Gaalen, S.M., Kruyt, M.C., Geuze, R.E., de Bruijn, J.D., Alblas, J., and Dhert, W.J., *Use of fluorochrome labels in in vivo bone tissue engineering research*. *Tissue engineering Part B: Reviews*, 2010. 16(2): p. 209-217.
46. Lian, J.B. and Stein, G.S., *Development of the osteoblast phenotype: molecular mechanisms mediating osteoblast growth and differentiation*. *The Iowa orthopaedic journal*, 1995. 15: p. 118.
47. Hong, D., Chen, H.-X., Yu, H.-Q., Liang, Y., Wang, C., Lian, Q.-Q., Deng, H.-T., and Ge, R.-S., *Morphological and proteomic analysis of early stage of osteoblast differentiation in osteoblastic progenitor cells*. *Experimental cell research*, 2010. 316(14): p. 2291-2300.
48. Pacifici, M., Golden, E.B., Oshima, O., Shapiro, I.M., Leboy, P.S., and Adams, S.L., *Hypertrophic Chondrocytes*. *Annals of the New York Academy of Sciences*, 1990. 599(1): p. 45-57.

ABSTRACT

Background: Suture expansion is a very important clinical approach to correct maxillary width deficiency, but it has a high potential for treatment relapse. Accelerating bone formation and mineralization in the midpalatal suture during suture expansion is beneficial in preventing relapse of the arch width and reducing the retention period. Pyk2 is tyrosine kinase which has been shown to mediate signaling pathways that are involved in the process of bone remodeling. Pyk2 knock-out (KO) mice have augmented bone formation and increased bone mass, suggesting that therapeutic strategies that inhibit Pyk2 may be useful to enhance bone remodeling and prevent suture relapse during suture expansion.

Objectives: To determine if Pyk2-deficiency affects midpalatal suture bone mass and bone remodeling with or without suture expansion in mice.

Methods: Thirty-six Pyk2-KO and thirty-six wild type (WT) 6 week-old male mice were randomly assigned into three groups: receiving no expansion force (0 g), 10 g or 20 g force of rapid maxillary expansion for 14 days. Half of the mice in each group were used for histology analysis; the other half was assigned for fluorescence analysis. Suture width, maxilla width and bone volume/tissue volume around suture bone edges were measured using micro-CT. Histological analyses of osteoclasts (tartrate resistant acid phosphatase, TRAP), osteoblasts (alkaline phosphatase, ALP) and chondrocytes (alcian blue) were performed.

Results: The BV/TV ratio was significantly higher in Pyk2-KO control mice compared to WT control mice. Suture expansion in WT and Pyk2-KO mice led to an increase in bone marrow spaces around the suture edge and significantly reduced BV/TV. Expansion also led to a significant increase in suture width, suture fibrous area, osteoclast

number, cartilage area and hypertrophic chondrocyte number. However, BV/TV in Pyk2-KO mice was significantly higher than in WT mice at both the 10 g and 20 g force levels. In addition, Pyk2-KO exhibited reduced suture width, maxilla width, fibrous area and osteoclast number per bone surface (OC.S/BS) compared to WT mice under expansion forces. Cartilage area and hypertrophic chondrocyte number were increased by force but were independent of mouse genotypes.

Conclusion: Pyk2-KO mice have higher BV/TV and narrower suture width compared to WT mice, which may be due to decreased osteoclast activity. The higher BV/TV of the midpalatal sutures of Pyk2-KO mice following suture expansion may suggest the presence of a more stable suture that has a reduced potential for relapse. Therapeutic strategies to inhibit Pyk2 during RME may be beneficial in increasing bone mass and preventing relapse of the suture.

ABBREVIATIONS

ALP	Alkaline Phosphatase
BMP-2	Bone Morphogenetic Protein-2
BV/TV	Bone Volume to Tissue Volume
H&E	Hematoxylin and Eosin
IHC	Inmmunohistochemistry
IL-1	Interleukin-1
Pyk2-KO	Knock Out
MMA	Methyl Methacrylate
Ni-Ti	Nickel-Titanium
Oc.S/BS	Osteoclast Surface to Bone surface
OPG	Osteoprotegerin
Pyk2	Proline-rich tyrosine Kinase 2
RANKL	Receptor Activator of the NF-KB Ligand
RME	Rapid Maxillary Expansion
rhBMP-2	Recombinant Human Bone Morphogenetic Protein-2
ROI	Regions of Interest
TGF- β	Transforming Growth factor- β
TNF	Tumor Necrosis Factor
TRAP	Tartrate Resistant Acid Phosphatase
VEGF	Vascular Endothelial Growth Factor
WT	Wide Type

CURRICULUM VITAE

BIOGRAPHICAL SKETCH

NAME Jun Sun	POSITION TITLE Graduate Prosthodontics Residency, Indiana University School of Dentistry
eRA COMMONS USER NAME (credential, e.g., agency login) junsun	

EDUCATION/TRAINING (*Begin with baccalaureate or other initial professional education, such as nursing, include postdoctoral training and residency training if applicable.*)

INSTITUTION AND LOCATION	DEGREE	MM/YYYY	FIELD OF STUDY
Sichuan University, Chengdu, Sichuan, China	D.D.S.	07/1994	Dentistry
Sichuan University, Chengdu, Sichuan, China	M.S.	07/1997	Prosthodontics
Sichuan University, Chengdu, Sichuan, China	Ph.D.	07/2003	Prosthodontics
Indiana University, Indianapolis, IN	Postdoc	03/2008	Oral Biology
Indiana University, Indianapolis, IN	Postdoc	10/2010	Orthodontics
Indiana University, Indianapolis, IN	M.S.D.	08/2015	Prosthodontics

A. Personal Statement

The goal of the proposed study is to investigate the bone formation and suture remodeling in the midpalatal suture created by rapid maxillary expansion with global Pyk2-deficiency mice. Alternative hypothesis is that Pyk2-deficiency will increase midpalatal suture bone formation following suture expansion. If our study results support the hypothesis, there is great potential of Pyk2 gene for clinical application. With inhibitor of Pyk2, the pharmaceutical aid could be therapeutically beneficial to the inhibition of relapse and shortening of retention period during rapid midpalatal suture expansion. During three years research work as a postdoctoral fellow in IUSD, I successfully carried out different projects on animal study, cytobiology and molecular biology studies *in vitro* and *in vivo*. Especially, I can conduct Micro-CT and histologic experiments after the training in Mineralized Tissue and Histology Research Laboratory of Orthodontic Department. The research team of Dr. Bruzzaniti has devoted to the study of mechanism of Pyk2 signaling pathway and acquired great achievement. I believe that my broad background in dental clinical and research training has prepared me to conduct the proposed project with Dr. Bruzzaniti's guidance.

B. Positions

Positions and Employment

2012- Graduate Prosthodontics Resident, Department of Prosthodontics, Indiana University School of Dentistry, Indianapolis, IN

2010- Postdoctoral fellow, Department of Orthodontics and Oral Facial Genetics, Indiana University School of Dentistry, Indianapolis, IN

2008- Postdoctoral fellow, Department of Oral Biology, Indiana University School of Dentistry, Indianapolis, IN

1997- Faculty, Sichuan University School of Dentistry, Chengdu, Sichuan, China

Other Experience and Professional Memberships

2012- Member, American College of Prosthodontics

2010- Member, Indiana Section of the American Association for Dental Research

C. Selected Peer-reviewed Publications

Most relevant to the current application

1. Liu SS, Xu H, Sun J, et al. Recombinant human bone morphogenetic protein-2 stimulates bone formation during interfrontal suture expansion in rabbits. *Am J Orthod Dentofacial Orthop.* 2013;144(2):210-7
2. Sun J, Song F, Zhang W, et al. Effects of alendronate on human osteoblast-like MG63 cells and matrix metalloproteinases. *Arch Oral Biol.* 2012;57(6):728-36
3. Liu SS, Cruz-Marroquin E, Sun J, et al. Orthodontic mini-implant diameter does not affect in-situ linear microcrack generation in the mandible or the maxilla. *Am J Orthod Dentofacial Orthop.* 2012;142(6):768-73.
4. Liu Y, Song F, Sun J, et al. Suture compression induced bone resorption with intensified MMP-1 and 13 expressions. *Bone.* 2012;51(4):695-703
5. Saini P, Al-Shibani N, Sun J, et al. Effects of *Calendula officinalis* on human gingival fibroblasts. *Homeopathy.* 2012;101(2):92-8.
6. Sun J, Weng Y, Song F, et al. In vitro responses of human pulp cells and 3T3 mouse fibroblasts to six contemporary dental restoratives. *J Biomed Sci Eng* 2011;4(1):18-28

Additional recent publications of importance to the field (in chronological order)

1. Sun J, Luo Y, Chao Y. Effect of thickness and shade of porcelain of ceramometal restorations on color of gingival porcelain. (PMID:16078471) *West China Journal of Stomatology.* 2005; 23(3):251-253

2. Sun J, Wang M, Chao Y. Effect of thickness on the color of denture resins. *Journal of Oral Science research*. 2005;21(3):262-264.
3. Sun J, Chao Y. Influences of esthetic prosthesis on gingiva (Review). *Foreign Medical Sciences*, 2005;32(3): 219-221.
4. Sun J, Zhao K, Cheng X. Effect of denture adhesives on masticating function. *Acta Universitatis Medicinalis Nanjing (Natural science)*. 2003;23(2):161-162
5. Sun J, Chen X, Liao Y. Effect of heat treatment on fracture toughness of dental glass ceramic. *Chinese Journal of prosthodontics*. 2003;4(1):11-12
6. Sun J, Chen X, Zhao Y. Effect of crystallizing temperature on microstructure and mechanical properties of dental glass ceramic. *Journal of Dental Research*, 2003;82 (Spec IssC): C-363

D. Award

2015 Delta Dental Foundation – Dental Master’s Thesis Award